Eurasian Chemical Communications (ECC)

Volume No. 6

Issue No. 1

January - April 2024

ENRICHED PUBLICATIONS PVT. LTD

S-9, IInd FLOOR, MLU POCKET,
MANISH ABHINAV PLAZA-II, ABOVE FEDERAL BANK,
PLOT NO-5, SECTOR-5, DWARKA, NEW DELHI, INDIA-110075,
PHONE: - + (91)-(11)-47026006

Eurasian Chemical Communications (ECC)

Aims and Scope

Eurasian Chemical Communications (ECC) publishes experimental, theoretical and applied research papers related to all branches of Chemistry. The world of the Internet is a multi-faceted one. Each and every field of Internet is witnessing tremendous growth in the present century. But , researchers still have to wait for a long time to publish their research articles in reputed journals. To tide over this disadvantage, we have launched this online research journal.

All papers submitted to Eurasian Chem. Commun. are subjected to peer review. All contributions in the following forms are invited

SUBJECTS AREA

Related subjects:

1. Analytical Chemistry
2. Biochemistry & Biophysics
3. Inorganic Chemistry
4. Organic Chemistry
5. Physical Chemistry
6. Effects of Chemical Drugs
7. Medicinal Studies of Synthetic Drugs
8. Pharmaceutical Chemistry
9. Neurochemical Research
10. Clinical Chemistry
11. Chemical Pathology
12. Computational Chemistry
13. Mathematical chemistry

All Fields Related to Chemical Science

All papers submitted to Eurasian Chem. Commun. are subjected to peer review. All contributions in the following forms are invited

(a) Original Research Articles
(b) Review Articles
(c) Short Communications

Contact Us

E-Mail: ss.sajjadifar@gmail.com (Dr. Sami Sajjadifar, Owner & Director-in-Charge)
Tel & Fax number:+98 (84) 32226101
ECC Editorial Office (Miss. Panahi): panahi.maryam406@yahoo.com

Eurasian Chemical Communications (ECC)

Eurasian Chemical Communications (ECC)

(Volume No. 6, Issue No. 1, January - April 2024)

Contents

The Convergence of IFRS and its Impact on the Stock Market Performance of the Jewelry Industry

Samrudha Nayak[*1], B. C. M. Patnaik[2], Ipseeta Satpathy[3]
[1,2,3]School of Management, KIIT University, Bhubaneswar, Odisha
*Corresponding Author: Email - samrudha.nayak95@gmail.com, Tel.:+91 7205027515

ABSTRACT

We analyzed the effect of combining with IFRS on the stock market performance of selected jewelry organizations recorded in S&P BSE 100. The period of seven years from 2013 to 2019 was chosen and Ordinary Least Square (OLS) regression model was utilized for the examination. The results revealed that the worth of financial statements was high on converging with IFRS. The effect of budget (financial) report factors on the Indian Stock Market was proved to be evident regarding PAT. Be that as it may, all financial variables showed a huge relationship with securities exchange market indicators.

KEYWORDS : Indian financial reporting standard; jewelry organizations; convergence of Indian financial reporting standard; stock market; performance; financial statements.

INTRODUCTION

As we know that change is the only constant, hence the accounting policies also transformed from ancient traditional systems to modern systems. Due to globalization and competition among the countries for attaining leadership at the economic front and to present their organizations globally, there is a need for more and more funds. The adoption of global accounting standards helps to raise capital from foreign markets and compete with other countries. If we intend to raise capital compared with the country of origin where our entity operates, we need to understand the accounting rules and regulations of that country from which we plan to raise capital. In this scenario, we cannot isolate ourselves from the rest of the world and the developments taking place around us. This led to the need for the International Financial Reporting Standards (IFRS). During the period of late Dr. Pranab Mukharjee, as Finance Minister of India, IFRS adopted India with the Indian version of accounting standards. This convergence resulted in IndAS. This helps to bring about uniformity, rationalization, comparability, transparency, and adaptability of financial statements. This also facilitates the cross-border flow of money, global listing in different stock exchanges, and eliminates the cost of reinstatement of financial statements.

A positive response to IFRS implementation was received from firms already equipped with excellent pre-adoption data [1]. The adjustments in the stock cost, after the IFRS adoption, in various industries were found. Co-development of stock cost diminished after embracing IFRS and the extent of the effect of IFRS appropriation varied from company to company [2]. In line with the discoveries from an overview of literature by hook (2018), IFRS has improved the straightforwardness and commonality of financial statements through point by point exposures [3].

Regarding the effect of the adoption of IFRS on the speculator's financial presentation in securities exchanges, we found that in the post-IFRS environment, the resilience of stock return to risks had been higher [4]. There exists an opposite view to some earlier researches that IFRS adoption guarantees better

accounting data. They believed that there was a strong aversion to acceptance and adoption of IFRS from several business organizations [5]. With the assistance of financial ratios and accounting figures, contrasts between local GAAP and IFRS-based budget reports and the impact of IFRS on the budgetary account of 140 organizations whose stocks were traded on the Istanbul Stock Exchange, Turkey were found. They uncovered that the financial statements computed as per GAAP and IFRS were measurably extraordinary. These critical contrasts were recognized to be existing in inventories, fixed assets, long-term liabilities, and investors' equity accounts [6]. The union of Indian Accounting Standards and IFRS impact on Multinational Enterprises and giant global accounting firms could deliberately tamper with accounts related to monetary assets to suit their interests, in total disregard to the interests of the public. Similarly, the effect of IFRS on 238 organizations was investigated in Greece. It was found that IFRS significantly affected the financial position of those organizations and announced execution just as on equipping and liquidity [7]. Overall, the effect on shareholders' value and total compensation was positive, while the impact on liquidity was negative. In any case, the significant effect on liquidity and overall gain was experienced by organizations with examiners other than the Big4 evaluating and auditing firms [8]. The priority to run a business effectively is to have a decent financial reporting framework set up [9]. Accounting professionals and accounting bodies over the globe, from a decade ago, have attempted to set up a financial reporting framework that is blended, vigorous, and has broad applicability. There were market responses to the first-time adoption of IFRS [10]. Using Tobin's Q, researchers have examined the impact of the implementation of IFRS on Chinese organizations. Their examination did not discover considerable contrasts in the mean and median of Tobin's Q after the usage of IFRS. Instead, there was a substantial contrast in the standard deviation [11]. They reasoned that a year-by-year examination of the change neglected to uphold the desire that IFRS caused the expansion in the standard deviation [12].

THE OBJECTIVE OF THE STUDY

The current study aimed at studying the effect of IFRS implementation on the stock exchange of the selected jewelry organization and proposing suggestions, if any, based on the findings.

Hypotheses of the study

H1: Adoption of IFRS by the sample gallery organizations has no impact on their stock market performances.

H2: IFRS-conformed financial reportings of sample jewelry companies have a financial impact on their stock market performances.

THE METHODOLOGY OF THE STUDY

The study examined the financial data of 10 jewelry organizations recorded in S&P BSE100, which had embraced IFRS, with impact-analysis from April 01, 2016. Table 1 gives the rundown of 10 jewelry organizations, chosen for this investigation. The time of the examination was seven years, from 2013 to 2019, including three years pre IFRS period from 2013 to 2015 and three years of the post-IFRS period from 2016 to 2019. The nitty-gritty separation of the examination time frame is given beneath in Table 2. The necessary information for this investigation was taken from CMIE-Prowess information bases.

TABLE 1 List of sample companies

Sl. No.	Company's name	Sector
1	Tanishq	Jewelry Organization
2	Atlas Jewellery	Jewelry Organization
3	Reliance Jewels	Jewelry Organization
4	Malabar Gold and Diamonds	Jewelry Organization
5	PC Jewellers	Jewelry Organization
6	Uday Jewellery	Jewelry Organization
7	Goenka Diamonds	Jewelry Organization
8	Kalyan Jewellers	Jewelry Organization
9	Swarnasarita	Jewelry Organization
10	Senco Gold and Diamonds	Jewelry Organization

TABLE 2 Period of the study

Period of the study	Break up of years
01.04.2013 TO 31.03.2014	PRE IFRS PERIOD
01.04.2014 TO 31.03.2015	PRE IFRS PERIOD
01.04.2015 TO 31.3.2016	PRE IFRS PERIOD
01.04.2016 TO 31.03.2017	POST IFRS PERIOD
01.04.2017 TO 31.03.2018	POST IFRS PERIOD
01.04.2018 TO 31.03.2019	POST IFRS PERIOD
01.04.2019 TO 31.03.2020	POST IFRS PERIOD

FACTORS AND TOOLS UTILIZED IN THIS STUDY

This examination utilized four fundamental factors to gauge the effect on securities exchange execution, in connection with the IGAAP and IFRS financial reporting by sample jewelry organizations. The four factors were Price to Book Ratio, Return on Equity, Profit after Tax, and Cash flow from Operations. With the end goal of the investigation and for testing the theory, the examination relied on tools like descriptive statistics, correlation, and OLS regression was utilized [16]. The investigation utilized key factors like Return on Equity, Profit after Tax and Cash flow from activities of financial statements and summaries that included Balance Sheet, Profit And Loss Statement, and Cash Flow Statement. The stock market performance of the sample organizations was inspected by utilizing Price to Book proportion. The OLS regression equation, utilized in this investigation, is given as follows:

$$P/B_{it}=\beta+\beta 1ROE_{it}+\beta 2CFO_{it}+\beta 3PAT_{it}+\varepsilon_{it}$$

Where,

P/B_{it} is the ratio of market price per share to book value per share of the i^{th} company of the financial year t

CFO_{it} is the net cash flow from operating activities of the i^{th} company of the financial year t

ROE_{it} is the return on net worth or equity of the i^{th} company as at the end of the financial year t

PAT_{it} is the profit after tax of the i^{th} company for the financial year t

ε_{it} is the error term which is assumed to have a 0 mean and constant variation

$\beta 1, \beta 2, \beta 3, \beta 4$ are slope coefficients

β is the regular term.

RESULTS OF THE STUDY

The post effects of descriptive statistics demonstrating the attributes of sample ratios, arranged by utilizing IGAAP and IFRS, for the example time of seven years are introduced in Table-3. It is worth noting that the Price to Book ratio was the variable used to quantify the securities exchange execution and stock market performance. ROE, CFO, and PAT were the financial statement factors. The mean

estimation of cost to book ratio of 5.28, during pre-IFRS and post-IFRS, demonstrated a decrease in the mean an incentive at 5.04, after joining with IFRS by the sample firms. The standard deviation went from 2.50 to 2.37 during the pre and post IFRS period, which additionally demonstrated a declining pattern. The Return on Equity ranged from the mean of 2.01 and standard deviation of 0.83 during the pre-IFRS period to the mean estimation of 3.30 and standard deviation of 3.12 during the post-IFRS period showed a slanting pattern of ROE on converging with IFRS. Correspondingly, the CFO ranged from a me9an estimation of 8019.05 and standard deviation estimation of 6568.99 during the pre-IFRS period, to a mean estimate of 8972.72 and standard deviation estimation of 9224.07 during the post-IFRS period, which demonstrated a positive increment in the income on uniting with IFRS. At last, the profit after tax extended from a mean estimation of 8730.34 and standard deviation estimate of 6654.84 during the pre-IFRS period, to a mean estimate of 8995.52 and standard deviation estimation of 7745.14 during the post-IFRS period, showing a slanting pattern of the PAT on meeting with IFRS. Accordingly, it is reasoned that all three factors (ROE, PAT, and CFO) had a constructive effect on meeting with IFRS while the P/B ratio indicated a negative impact on joining with IFRS. The examination of skewness showed that all the estimations of sample organizations against sample factors were positive, which suggested that it was correctly followed. Be that as it may, the kurtosis values for all sample firms, against sample factors were seen to be more prominent than the three ones which demonstrated extraordinary leptokurtic distribution.

TABLE 3 Results of descriptive statistics for sample variables during the period 2013-2020

Variables	Mean	Standard Deviation	Minimum	Maximum	Skewness	Kurtosis
Pre IFRS period (2012-2015)						
Price to Book Ratio	5.28	2.50	0.83	17.03	2.36	4.76
Return on Equity	2.01	0.83	0.25	1.95	0.12	4.42
Cash Flow from Operations	8019.05	6568.99	1264.80	28815.20	1.95	5.64
Profit After Tax	8730.34	6654.84	486.10	38285.50	2.23	0.99
Post IFRS period (2016–2020)						
Price to Book Ratio	5.04	2.37	0.80	9.28	0.29	5.41
Return on Equity	3.30	3.12	0.37	19.21	0.26	9.45
Cash Flow from Operations	8972.72	9224.07	98.60	43796.10	2.92	6.59
Profit After Tax	8995.52	7745.14	268.40	31813.30	2.13	7.94

Source: Compiled from Prowess Database and computed using SPSS

Table 4 shows the post effects of connection between sample factors, i.e. P/B, ROE, PAT, and CFO. As expressed before, the P/B ratio symbolizes the securities exchange execution, and the other three factors, i.e. ROE, PAT, and CFO symbolize the budget summary, arranged under IGAAP and IFRS. The consequences of connection unmistakably showed that there was a negative relationship with the Price to Book Ratio during the pre- IFRS period, at - 0.081, and during the post-IFRS period at -0.025. As such, there was a converse connection between ROE and Price to Book Ratio. Also, there was a specific high relationship between the Price to Book Ratio and Profit after duty during the pre-IFRS period in 0.683 and the post-IFRS period in 0.119. Likewise, the connection between the cost to book proportion and cash flows from operations was exceptionally certain, at 0.414, during the pre-IFRS period and with 0.213, during the post-IFRS period. Thus, it is perceived that all three financial statement factors, i.e.

ROE, CFO, and PAT had impacts over the securities exchange execution and stock market performance variable, i.e. P/B proportion during the investigation time frame.

TABLE 4 Results of correlation analysis for sample variables during the period 2012-2020

Variables	Price to Book Ratio	Return on Equity	Cash Flow from Operations	Profit After Tax
Pre IFRS period (2012–2015)				
Price to Book Ratio	1	-0.081	0.414*	0.683*
Return on Equity	-0.081	1	-0.176	0.071
Cash Flow From Operations	0.414*	-0.176	1	0.687
Profit After Tax	0.683*	0.071	0.687	1
Post IFRS period (2016–2020)				
Price to Book Ratio	1	-0.025	0.213	0.119*
Return on Equity	-0.025	1	-0.280	-0.350*
Cash Flow,From Operations	0.213	-0.280	1	0.588*
Profit After Tax	0.119*	- 0.350*	0.588*	1

*Correlation is significant @ 5%

Source: Compiled from Prowess Database and computed using SPSS

The results of Table 5 show the effect of IFRS on financial statements, arranged by utilizing IGAAP and IFRS, and on the stock market performance of the sample jewelry organizations, recorded in S&P BSE100. The OLS regression examination was used to contemplate the financial effect of IFRS on the stock market performance of the sample firms, during IGAAP revealing norm and IFRS detailing principles. The P/B proportion was considered as the dependent variable and ROE, PAT, and CFO as the autonomous factors, symbolizing the financial statements of IFRS and IGAAP in this examination. The results of the financial-related effect of merging with IFRS over the stock market performance of sample firms, during the examination time frame from April 01, 2013, to March 31, 2020, are summed up in Table 6, which delineates that the estimations of coefficients, for the year 2012, were at -1.957, -0.625 and 0.526 for ROE, CFO, and PAT, with a consistent estimate of 6.857, regarding sample firms. As indicated by the results of coefficient esteems, a positive effect on securities exchange execution was made by a Profit After Tax (PAT) and a negative impact by two factors, in particular, ROE and CFO, concerning test firms for the year 2013. For the year 2014, the coefficient estimates were accounted for as - 0.208, 0.421, and 0.361, for ROE, CFO, and PAT, with an estimation of steady at 2.990. A positive effect on stock market performance was observed on account of CFO and PAT and an adverse effect for ROE, in the year 2014. The year 2015 coefficient accounted for as 0.156, -0.428, and 0.626, for ROE, CFO, and PAT individually with an estimation of steady 2.893. A positive effect on securities exchange execution was seen on account of ROE and PAT, and a negative impact for CFO was likewise recorded in 2014. From the above examination, plainly during the pre-IFRS period, budgetary factors, arranged by utilizing IGAAP, a variable of PAT demonstrated a critical positive effect on the securities exchange execution.

TABLE 5 Result of regression analysis of sample variables for the period of 2012-2020

Year	Constant	ROE	CFO	PAT	AdjR2	F-Stat	P-Value
Pre IFRS period (2012–2015)							
2013	6.857	-1.957	-0.625	0.526	0.664	1.687	0.488
2014	2.990	-0.208	0.521	0.461	0.624	3.912	0.704
2015	2.893	0.156	-0.428	0.626	0.864	3.796	0.075
Post IFRS period (2016–2020)							
2016	2.709	0.256	0.479	0.097	0.164	0.662	0.696
2017	4.814	-0.152	1.137	1.117	0.477	0.434	0.068
2018	6.376	-0.272	-0.697	0.487	0.882	1.358	0.337
2019	7.456	0.756	1.768	0.577	0.989	3.976	0.987

Source: Compiled from Prowess Database and computed using SPSS

Like the post-IFRS time of 2016, the coefficient values were accounted for as 0.152, 0.479, and 0.097, for ROE, CFO, and PAT separately, with an estimation of consistency at 2.709. A positive effect on stock market performance was evident on account of the apparent multitude of three factors like ROE, CFO, and PAT, during the year 2016. Correspondingly, for the year 2017, the coefficient values were accounted for as -0.152, 1.137, and 1.117 for ROE, CFO, and PAT individually with an estimation of consistency at 4.814. It is apparent that the CFO and PAT had made substantial positive effects, and ROE had an adverse impact on the stock exhibition of sample firms. In 2018, the coefficient values were recorded as -0.272, -0.697, and 0.477, for ROE, CFO, and PAT individually, with an estimation of steady at 6.376. The factors, for example, CFO and PAT, indicated a nearly certain effect, and one variable, ROE, demonstrated a negative impact on the stock market performance of the sample factors. Consequently, it is perceived that PAT left essentially certain effects on the securities exchange execution of the sample organizations. Subsequently, the null hypothesis (H1) stating there lies no connection between the money related result of uniting to IFRS by the sample gallery organizations over its securities exchange execution was rejected.

It should be noted that F-statistic, p-value, R-squared, and Adjusted R-squared were utilized to test the fitness of the regression model. In the year 2013, the Adjusted R-squared was 0.164 and the F value was 1.687, from which it is perceived that only 16.4% of the variance in P/B ratio could be estimated through this model in 2013. For the year 2014, the Adjusted R-squared was 0.434, and F esteem was 3.912, which inferred that 42.4% variety in P/B ratio could be estimated by utilizing this model in 2014. In the year 2015, the Adjusted R-squared was 0.664, and the F value was 3.796, which could clarify 56.4% of the variance in the P/B ratio. During the post-IFRS period in 2016, the Adjusted R-squared was 0.164, and the F value was 0.662, which implied that only 14.4% of the variance in P/B proportion utilized this model in 2016. In 2017, the Adjusted R-squared was at 0.477, and the F value was 3.424 which showed that 43.7% of the variance in P/B proportion could be clarified through this model for 2017. In 2018 the Adjusted R-squared was 0.882, and the F value was 1.358. It was discovered that in 2018, 81.2% variety in P/B proportion was estimated by this model. This affirmed that the model was acceptable, and the factors were freely appropriated.

CONCLUSION

This study examined the factors of financial statements, arranged by utilizing GAAP and IFRS, and attempted to discover relations with the securities market performance of the sample Jewellery organizations recorded in S&P BSE100. Four primary factors, to gauge the financial effect of IFRS on the stock exchange execution of the sample Jewellery organizations were used. There were four factors - Price to Book Ratio (securities exchange variable), Return on Equity, Profit after Tax and Cash flow from Operations (three monetary factors), utilized by this examination. The post effects of this examination showed that the financial effect after converging with IFRS, significantly Profit after Tax, was fundamentally indicative of the stock returns in Indian [13]. The results of this examination are unique, concerning numerous global investigations, although they looked predictable[14].

There were some limitations. The investigation focused only on jewelry organizations, and consequently, it is tough. Besides, this examination did not use estimated accrual methodology to look at the effect of financial statements or reports, which demanded a change in research configuration, as utilized in the current investigation. Some different proposals for additional exploration fit in this area. The present work could have reached out by fusing accounting gatherings and the nature of accounting divulgence [15].In conclusion, it is recommended that the examination configuration, utilizing

alternative dependent variables, e.g., stock returns, Tobin q, and panel data regression, could be used, contrasting the outcomes and OLS regression [16].

ACKNOWLEDGMENTS

This paper would not have been possible without the exceptional support of Dr.B.C.M. Patnaik, KIIT School of Management, KIIT University, Bhubaneswar, Odisha, India. His enthusiasm, knowledge, and exacting attention to detail have been an inspiration and kept my work on track from my first encounter with the logbooks of IFRS to the final draft of this paper. I also appreciate Jagat Jyoti Amar Singh, my colleague at KIIT University, who looked over my transcriptions and answered with unfailing patience numerous questions about the language of this article. My sincere gratitude goes to my RSC member Dr. Ipseeta Satapathy, Senior Professor, KIIT School of Management, KIIT University, Bhubaneswar, Odisha, India. The generosity and expertise of her improved this study in innumerable ways and saved me from many errors; those that inevitably remain are entirely my responsibility.

CONFLICTS OF INTEREST

We declare that there are no conflicts of interest regarding the publication of this manuscript.

Orcid:

Samrudha Nayak:
https://orcid.org/0000-0002-7698-6510

B.C.M. Patnaik:
https://orcid.org/0000-0002-5979-0989

IpseetaSatpathy:
https://orcid.org/0000-0002-0155-5548

REFERENCES

[1] E. Abbasi, Archives of Business Research, 2016, 4, 43-58.
[2] E. Adedayo, O. Foluke, O. Paul, International Journal of Accounting Research, 2018, 3, 23-34.
[3] B. Agyei-Mensah, International Journal of Accounting and Financial Reporting, 2014, 3, 269-278.
[4] M. Dvořák, L. Vašek, Procedia Economics and Finance, 2015, 25, 156-165.
[5] C. Ezeagba, Journal of Policy and Development Studies, 2017, 11, 21-42.
[6] H. Garrouch, M. Hadriche, A. Omri, International Journal of Managerial and Financial Accounting, 2014, 6, 322-339.
[7] M. Harris, K. Muller, J. Account. Econ., 1999, 26, 285-312.
[8] C. Haslam, Accounting, Economics, and Law: A Convivium, 2017, 7, 105-108.
[9] J. Hoon Yuk, W. Bin Leem, Investment Management, and Financial Innovations, 2017, 14, 243-250.
[10] Y. Kitamura, Asia-Pacific Financial Markets, 2010, 18, 1-31.
[11] D. Mbir, O. Agyemang, G. Tackie, M. Abeka, Cogent Bus. Manag., 2020, 7, 321-333.
[12] D. Ngoc Hung, P. Duc Cuong, V. Thi Bich Ha, Investment Management and Financial Innovations, 2018, 15, 210-218.
[13] M. Nnadi, Global Business and Economics Review, 2015, 17, 399-411.
[14] E. Olayinka, E. Emoarehi, O. Paul, International Journal of Accounting Research, 2017, 2, 52-61.
[15] I. Radikoko, E. Ndjadingwe, International Journal of Innovation and Economic Development, 2015, 1, 24-37.
[16] A. Salisu, T. Oloko, O. Oyewole, Borsa Istanbul Review, 2016, 16, 210-218.

How to cite this article:

Samrudha Nayak*,
B.C.M. Patnaik, Ipseeta Satpathy. The convergence of IFRS and its impact on the stock market performance of the jewelry industry. Eurasian Chemical Communications, 2021, 3(1), 6-13. Link:http://www.echemcom.com/artic le_119929.html

Weighted Entropies of $Tuc_5c_8[P;Q]$ Nanotube with the Degree based Topological Indices as Weights

Farkhanda Afzal[a], Faiza Afzal[b], Deeba Afzal[b,*], Mohammad Reza Farahani[c], Murat Cancan[d], Süleyman Ediz[d]

[a]MCS, National University of Sciences and Technology, Islamabad, Pakistan
[b]Department of Mathematics and Statistics, The University of Lahore, Lahore, 54000, Pakistan
[c]Department of Applied Mathematics, Iran University of Science and Technology, Tehran, Iran
[d]Faculty of Education, Van Yuzuncu Yıl University, Zeve Campus, Tuşba, 65080, Van, Turkey
*Corresponding Author: Email - deebafzal@gmail.com, Tel.: +923351572532

ABSTRACT

The entropy of a graph is a function depending both on the graph itself and on a probability distribution on its vertex set. This graph function originated in the problem of source coding in information theory and was introduced by J. Krner in 1973. Although the notion of graph entropy has its roots in information theory, it was proved to be closely related to some classical and frequently studied graph theoretic concepts. In this article, we captured the symmetry present in the structure of molecular graph of nanotube. We computed entropies of $TUC_5C_8[p;q]$ nanotube taking some degree-based topological indices as edge weights.

KEYWORDS : Nanotube; topological indices; weighted entropy; Zagreb indices; Randić index.

INTRODUCTION

The entropy of a graph is a function depending both on the graph itself and on a probability distribution on its vertex set. This graph function originated in the problem of source coding in information theory and was introduced by J. Korner in 1973. Although the notion of graph entropy has its roots in information theory, it was proved to be closely related to some classical and frequently studied graph theoretic concepts. Chemical reaction network theory is an area of applied mathematics that attempts to model the behavior of real world chemical systems. Since its foundation in the 1960s, it has attracted a growing research community, mainly due to its applications in biochemistry and theoretical chemistry. It has also attracted interest of pure mathematicians due to the interesting problems that arise from the mathematical structures involved.

Topological indices are arithmetic numbers about a graph of the chemical molecules [1-13]. Each molecule is canonically represented by a set of topological indices. Topological descriptors are derived from hydrogen-suppressed molecular graphs. Here, we computed weighted entropies of $TUC_5C_8[p;q]$ using some degree based topological indices.

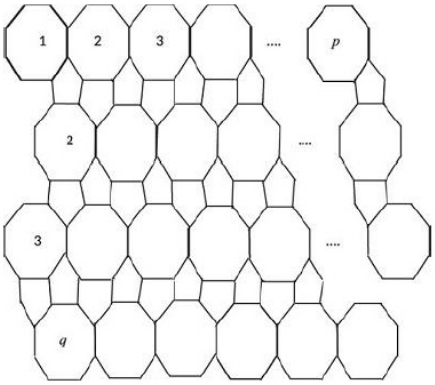

FIGURE 1 The 2-dimensional view of TUC5C8[p;q] nanotube.

Definition 1. (Entropy). Let the probability

$$\text{density function } P_{ij} = \frac{w(uv)}{\sum W(uv)}$$

then the entropy of graph G is defined as

$$I(G,w) = \sum P_{ij} \log P_{ij}.$$

TUC_5C_8[p;q] Nanotube

In the molecular graph of TUC5C8[p;q] with G=(V,E) there are two types of vertices in the graph G; namely degrees 2 and 3 as seen from the Figure 1.

Let G=(V,E) be the TUC5C8[p;q]. Note that here p denotes the number of C_5C_8 nets horizontally and q denotes the tube levels. The 2D lattice graph of TUC5C8[p;q] is shown in Figure 1.

There are 3 kinds of edges in TUC_5C_8[p;q] as follows.

E_1={uv∈E(TUC_5C_8)[p;q]: du=2;dv=2};
E_2={uv∈E(TUC_5C_8)[p;q]: du=3;dv=2};
E_3={uv∈E(TUC_5C_8)[p;q]): du=3;dv=3};
Such that $|E_1|$=2p;$|E_2|$=4p;$|E_3|$=6pq-2p.

Now from this edge partition, we can have following results immediately.

Entropies of TUC_5C_8[p;q] Nanotube

In this section we present our results.

Theorem 1. The entropy of TUC_5C_8[p;q] with first Zagreb weight is

$$I(TUC_5C_8[p,q],M_1) = log(36pq+16p) - \frac{1}{36pq+16p}[168.08067008pq - 9.4580650].$$

Proof. By Definition 1, we have

$$M_1(TUC_5C_8[p;q]) = 4p(9q+4);$$

$$I(TUC_5C_8[p,q],M_1) = log(36pq+16p)[|E_1|[(2+2)\times\log(2+2)] + |E_2|[(2+3)\times\log(2+3)] + |E_3[(3+3)\times\log(3+3)]$$

$$= log(36pq+16p) - \frac{1}{36pqq+16p}[(2p)[4\times log4] + (4p)[5\times log5] + (6pq-2p)[6\times\log 6]$$

$$= log(36pq+16p) - \frac{1}{36pq+16p}[(2p)\times[4log4] + (4p)[5log5] + (36pq)\times[6log6] - (2p)\times[6log6]$$

$$= log(36pq+16p) - \frac{1}{36pq+16p}[168.08067008pq - 9.45806501p].$$

Theorem 2. The entropy of $TUC_5C_8[p;q]$ with second Zagreb weight is

$$PI(TUC_5C_8[p,q],M_2) = log(54pq+14p) - \frac{1}{54pq+14p}[51.52909550pq - 7.6782692773p].$$

Proof. By Definition 1, we have

$$M_2(TUC_5C_8[p;q])=2p(27q+7);$$

$$I(TUC_5C_8[p,q],M_2) = log(54pq+14p) - \frac{1}{54pq+14}[|E_1|[(2.2)\times\log(2.2)]+|E_2|[(2.3) \times\log(2.3)]+|E_3|[(3.3)\times\log(3.3)]]$$

$$= log(54pq+14p) - \frac{1}{54pq+14}[(2p)(4\times\log 4) +(4p).(6\times\log 6)+(6pq-2p)(9\times\log 9)]$$

$$= log(54pq+14p) - \frac{1}{54pq+14}[2p(2.40823996) +(4p)(4.6689075027)(6pq-2p)(8.588182585)]$$

$$= log(54pq+14p) - \frac{1}{54pq+14}[4.81647992p +4.6689075027p+51.52909551pq -7.6782642773p]$$

$$= log(54pq+14p) - \frac{1}{54pq+14}$$

Theorem 3. The entropy of $TUC_5C_8[p;q]$ with second Modified Zagreb weight is

$$I(TUC_5C_8[p,q],^m M_2) = log(0.24p+1.6666pq) - \frac{1}{0.24p+1.6666pq}[-0.63616167pq - 0.005683629p].$$

Proof. By Definition 1, we have

$$^mM(TUC_5C_8[p;q])=0:24p+1:6666pq$$

$$I(TUC_5C_8[p,q],^m M) = log(0.24p+1.6666pq) - \frac{1}{0.24p+1.6666pq}[|E_1|[\frac{1}{2.2}\times\log\frac{1}{2.2}] +|E_2|[\frac{1}{2.3}\times\log\frac{1}{2.3}]+|E_3|[\frac{1}{3.3}\times\log\frac{1}{3.3}]]$$

$$= log(0.24p+1.6666pq) - \frac{1}{0.24p+1.6666pq} [(2p)(\frac{1}{4}\times\log\frac{1}{4})+(4p)(\frac{1}{6}\times\log\frac{1}{6}) +(6pq-2p)(\frac{1}{9}\times\log\frac{1}{9})]$$

$$= log(0.24p + 1.6666pq) - \frac{1}{0.24p + 1.6666pq}$$
$$[2p(-0.15051499783) + (4p)(-0.12969187506)$$
$$+(6pq - 2p)(-0.10602694549)]$$
$$= log(0.24p + 1.6666pq) - \frac{1}{0.24p + 1.6666pq}$$
$$[-0.30102999p - 0.518767500p$$
$$-0.63616167pq + 0.21205389p]$$
$$= log(0.24p + 1.6666pq) - \frac{1}{0.24p + 1.6666pq}$$
$$[-0.63616167pq - 0.005683629p].$$

Theorem 4. The entropy of TUC_5C_8 with Augmented Zagreb weight is

$$I(TUC_5C_8, AZ) = log(25.781p + 68.343pq)$$
$$-\frac{1}{25.781p + 68.343pq}[2.98539765pq - 16.3531868p].$$

Proof. By Definition 1, we have

AZ(TUC_{5}C_{8})=48p+22.78125p(3q-1),

$$I(TUC_5C_8, AZ) = log(25.781p + 68.343pq)$$
$$-\frac{1}{25.781p + 68.343pq}[|E_1|(\frac{2.2}{2+2-2^3})$$
$$\times \log(\frac{2.2}{2+2-2})^3] + [|E_2|(\frac{2.3}{2+3-2})^3$$
$$\times \log(\frac{2.3}{2+3-2})^3] + |E_3|[(\frac{3.3}{3+3-2})^3 \times \log(\frac{3.3}{3+3-2})^3]$$
$$= log(25.781p + 68.343pq) - \frac{1}{25.781p + 68.343pq}$$
$$[(2p)(2^3 \times \log 2^3)(4p)(2^3 \times \log 2^3)$$
$$+(6pq - 2p)(\frac{9}{4})^3 \times \log(\frac{9}{4})^3]$$
$$= log(25.781p + 68.343pq) - \frac{25.781p}{68.343pq}$$
$$[14.4494398p + 28.898879p + 2.98539765pq$$
$$-0.9965132p] = log(25.781p + 68.343pq)$$
$$-\frac{1}{25.781p + 68.343pq}[2.98539765pq - 16.3531868p]$$

Theorem 5. The entropy of $TUC_5C_8[p;q]$ with Hyper second Zagreb weight is

$$I(TUC_5C_8[p,q], H_2) = log(486pq + 14p)$$

$$-\frac{1}{486pq+14p}[927.5237pq-8.003334p].$$

Proof. By Definition 1, we have

$$H_2(TUC_5C_8[p,q]) = 486pq+14p,$$

$$I(TUC_5C_8[p,q],H_2) = \log(486pq+14p)$$

$$-\frac{1}{486pq+14p}[|E_1|\left[(2.2)^2\times\log(2.2)^2\right]$$

$$+[|E_2|[(2.3)^2\times\log(2.3)^2]+[|E_3|\left[(3.3)^2\times\log(3.3)^2\right]]$$

$$=\log(972pq-18p)-\frac{1}{972pq-18p}\left[(2p)\times4^2\log4^2\right.$$

$$\left.+(4p)\times6^2\log6^2+(6pq-2p)\times9^2\log9^2\right]$$

$$=log(486pq+14p)-\frac{1}{486pq+14p}[77.0636789p$$

$$+224.107560p+927.5237pq-309.174573p]$$

$$=log(486pq+14p)-\frac{1}{486pq+14p}$$

$$[927.5237pq-8.003334p].$$

Theorem 6. The entropy of $TUC_5C_8[p;q]$ with Redefined First Zagreb weight is

$$I(TUC_5C_8[p,q],ReZG_1) = log(216pq+60p)$$

$$-\frac{1}{216pq+60p}[-0.704365pq-0.029142p].$$

Proof. By Definition 1, we have

$$ReZG_1(TUC_5C_8[p,q]) = 216pq+60p,$$

$$I(TUC_5C_8[p,q],ReZG_1) = log(216pq+60p)$$

$$-\frac{1}{216pq+60p}[|E_1|\left[\frac{2+2}{2.2}\times\log\frac{2+2}{2.2}\right]$$

$$+[|E_2|\left[\frac{2+3}{2.3}\times\log\frac{2+3}{2.3}\right]+[|E_3|\left[\frac{3+3}{3.3}\times\log\frac{3+3}{3.3}\right]$$

$$=\log(216pq+60p)-\frac{1}{216pq+60p}[(2p).\left[\frac{4}{4}\times\log\frac{4}{4}\right]$$

$$+[(4p).\left[\frac{5}{6}\times\log\frac{5}{6}\right]+[(6pq-2p).\left[\frac{2}{3}\times\log\frac{2}{3}\right]$$

$$=\log(216pq+60p)-\frac{1}{216pq+60p}[-0.26393p$$

$$-0.704365pq+0.234788p]$$

$$=\log(216pq+60p)-\frac{1}{216pq+60p}$$

$$[-0.704365pq-0.029142p].$$

Theorem 7. The entropy of $TUC_5C_8[p;q]$ with Re-defined 2nd Zagreb weight is

$$I(TUC_5C_8[p,q],ReZG_2) = log(9pq-3.8p) - \frac{1}{9pq-3.8p}[1.58482133pq-0.1482037p].$$

Proof. By Definition 1, we have

$$ReZG_2(TUC_5C_8[p,q]) = 9pq-3.8p,$$

$$I(TUC_5C_8[p,q],ReZG_2) = \log(9pq-3.8p) - \frac{1}{9pq-3.8p}[|E_1|[\frac{2.2}{2+2}\times\log\frac{2.2}{2+2}]$$

$$+[|E_2|[\frac{2.3}{2+3}\times\log\frac{2.3}{2+3}]+[|E_3|[\frac{3.3}{3+3}\times\log\frac{3.3}{3+3}]]$$

$$= \log(9pq-3.8p) - \frac{1}{9pq-3.8p}[(0).[\frac{4}{4}\times\log\frac{4}{4}]$$

$$+[(4p).[\frac{6}{5}\times\log\frac{6}{5}]+[(12pq-2p).[\frac{3}{2}\times\log\frac{3}{2}]]$$

$$= \log(9pq-3.8p) - \frac{1}{9pq-3.8p}[0.38006998p$$

$$+1.58482133pq-0.52827377p]$$

$$= \log(9pq-3.8p) - \frac{1}{9pq-3.8p}$$

$$[1.58482133pq-0.1482037p].$$

Theorem 8. The entropy of $TUC_5C_8[p;q]$ with Re-defined 3rd Zagreb weight is

$$I(TUC_5C_8[p,q],ReZG_3) = log(324pq+44p) - \frac{1}{324pq+44p}[561.2955pq+28.687869p].$$

Proof. By Definition 1, we have

$$ReZG_3(TUC_5C_8[p,q]) = 324pq+44p,$$

$$I(TUC_5C_8[p,q],ReZG_3) = \log(324pq+44p) - \frac{1}{324pq+44p}[|E_1|[(2.2)(2+2)\times\log(2.2)$$

$$(2+2)]+|E_2|[(2.3)(2+3)\times\log(2.3)(2+3)]$$

$$+[|E_3|[(3.3)(3+3)\times\log(3.3)(3+3)]]$$

$$= \log(324pq+44p) - \frac{1}{324pq+44p}$$

$$\left[(2p)\times 16\log 16+(4p)\times 30\log 30\right.$$
$$\left.+(6pq-2p)\times 54\log 54\right]$$
$$=log(324pq+44p)-\frac{1}{324pq+44p}[38.531839p$$
$$+177.25455p-561.2955pq-187.09852p]$$
$$=log(324pq+44p)-\frac{1}{324pq+44p}$$
$$[561.2955pq+28.687869p].$$

ACKNOWLEDGMENTS

The authors would like to thank the reviewers for their helpful suggestions and comments.

Orcid:

Farkhanda Afzal:
https://orcid.org/0000-0001-5396-7598

Deeba Afzal:
https://orcid.org/0000-0001-5268-7260

Mohammad Reza Farahani:
https://orcid.org/0000-0003-2969-4280

Murat Cancan:
https://orcid.org/0000-0002-8606-2274

Süleyman Ediz:
https://orcid.org/0000-0003-0625-3634

REFERENCES

[1] F. Afzal, S. Hussain, D. Afzal, S. Razaq, J. Inf. Opt. Sci., 2020, 41, 1061–1076.
[2] M. Cancan, S. Ediz, H. Mutee-Ur-Rehman, D. Afzal, J. Inf. Opt. Sci., 2020, 41, 1117-1131.
[3] M. Cancan, S. Ediz, M.R. Farahani, Eurasian Chem. Commun., 2020, 2, 641-645.
[4] A.Q. Baig, M. Naeem, W. Gao, J.B. Liu, Eurasian Chem. Commun., 2020, 2, 634-640.
[5] F. Afzal, M.A. Razaq, D. Afzal, S. Hameed, Eurasian Chem. Commun., 2020, 2, 652-662.
[6] M. Alaeiyan, C. Natarajan, G. Sathiamoorthy, M.R. Farahani, Eurasian Chem. Commun., 2020, 2, 646-651.
[7] H. Yang, X. Zhang, J. D. Math. Sci. and Cryp., 2018, 21, 1495-1507.
[8] M. Imran, S.A. Bokhary, S. Manzoor, M.K. Siddiqui, Eurasian Chem. Communm., 2020, 2, 680-687.
[9] Z. Ahmad, M. Naseem, M.K. Jamil, Sh. Wang, M.F. Nadeem, Eurasian Chem. Commun., 2020, 2, 712-721.
[10] Z. Ahmad, M. Naseem, M.K. Jamil, M.K. Siddiqui, M.F. Nadeem. Eurasian Chem. Commun., 2020, 2, 663-671.
[11] M. Cancan, S. Ediz, M.R. Farahani, Eurasian Chem. Commun., 2020, 2, 641-645.
[12] A.Q. Baig, M. Naeem, W. Gao, J.B. Liu, Eurasian Chem. Commun., 2020, 2, 634-640.
[13] F. Afzal, M.A. Razaq, D. Afzal, S. Hameed, Eurasian Chem. Commun., 2020, 2, 652-662.
[14] B.Y. Yang, Y.N. Yen, Adv. Appl. Math., 1995, 16, 72-94.
[15] C.E. Shannon, Bell. System Tech. J., 1948, 27, 379-423.
[16] C.E. Shannon, W. Weaver, Univ. Illinois Press, Urbana., 1949, 17, 1-117.
[17] E. Trucco, Bull. Math. Biol., 1965, 18, 129-135.

[18] K. Xu, K.C. Das, S. Balachandran, MATCH Commun. Math. Comput. Chem., 2014, 72, 641-654.
[19] M.M. Dehmer, N.N. Barbarini, K.K. Varmuza, A.A. Graber, BMC Structural Bio., 2010, 10, 18-34.
[20] N.P. Rao, P.A. Laxmi, Appl. Sci., 2008, 2, 2443-2457.
[21] N. Rashevsky, Bull. Math. Biophys., 1955, 17, 229-235.
[22] S. Ji, X. Li, B. Huo, MATCH Commun. Math. Comput. Chem., 2014, 72, 723-732.

How to cite this article:

Farkhanda Afzal, Faiza Afzal, Deeba Afzal*, Mohammad Reza Farahani, Murat Cancan, Süleyman Ediz. Weighted entropies of Tuc_5c_8[P;Q] nanotube with the degree based topological indices as weights. Eurasian Chemical Communications, 2021, 3(1), 14-18. Link: http://www.echemcom.com /article_120281.html

CuO Nanoflowers Modified Glassy Carbon Electrode for the Electrochemical Determination of Methionine

Maryam Ebrahimi[a], Hadi Beitollahi[b,*]

[a]Department of Chemistry, Graduate University of Advanced Technology, Kerman, Iran

[b]Environment Department, Institute of Science and High Technology and Environmental Sciences, Graduate University of Advanced Technology, Kerman, Iran

*Corresponding Author: Email - h.beitollahi@yahoo.com, Tel.: +983426226613

ABSTRACT

This study reported the electrochemical sensor for sensitive determination of methionine based on CuO nanoflowers (CuO NFs) supported on glassy carbon electrode (GCE). Therefore, we utilized cyclic voltammetry (CV), chronoamperometry (CHA) as well as differential pulse voltammetry (DPV) for characterizing the sensor performance. This CuO NFs/GCE has been found to have very good electrochemical catalytic activity toward methionine oxidation. The oxidation overpotential of methionine decreased significantly and its oxidation peak current increased dramatically at CuO NFs/GCE. Moreover, the sensor showed a linear response for detecting methionine in the broad ranges from 1.0-300.0 μM with a low limit of detection (LOD) equal to 0.3 μM. Finally, we employed CuO NFs/GCE as a highly sensitive tool to analyze methionine in real sample (urine).

KEYWORDS : Electrochemical Sensor; voltammetric determination; nanosensors.

INTRODUCTION

It is widely accepted that methionine (α-amino-γ-methyl mercaptobutyric acid) is one of the sulfur-bearing mono-carboxylic amino acids as one of the supplies of sulfur in body, which is essentially responsible for biological methylation reaction as well as prevention of disorders in the skin, hair and nail [1]. Although methionine has been considered as one of the essential amino acids, it is not synthesized in body and thus may be readily provided from the food supplies so pharmaceuticals can be commercially provided in the market. In addition, it is crucial for forming the blood protein, globulin as well as albumin, contributes to the reduction of the level of cholesterol via elevating the lecithin generation in livers, and keeps the cells' normal growth [2]. This drug has been proposed to be helpful for curing acquired immune deficiency syndrome (AIDS)-related myelopathy [3] as well as different kinds of cancers [4]. Furthermore, it is found in the humans' fluids such as in the blood plasma [5,6], urine and serum [7]. However, abnormal concentrations of methionine largely cause the coronary artery disease in humans [8] as well as hypermethioninemia and hyper-homocysteinemia in the infants [9]. Consequently, variations in the concentrations of methionine in human fluids have correlation with numerous acute illnesses. Due to its clinical and physiological significance, the determination of methionine in human fluids is very important. Over the past years, many analytical methods have been developed to detect methionine like high-performance liquid chromatography (HPLC)[10], colorimetric [11,12], enzymatic [13], capillary electrophoresis–UV [6], photoelectrochemical [14], gas chromatography–mass spectrometry [15], spectrophotometric [16] and electrochemical techniques [17-19].

On the other hand, electrochemical sensors fulfil several needs specifically because of simplified preparation, higher sensitivity and selectivity and faster responses [20-31]. In case of the use of the

unmodified electrodes for detecting this analyte, many challenges like decreased sensitivity, slower electron transfer kinetics, duplicability, decreased stability on a wide range of solution compounds, as well as greater overpotential would occur, in which the electron transfer processes will be seen [32]. Nonetheless, chemical modification of the electrodes surfaces has been considered as one of the current approaches for designing the electrochemical sensors that is a developed strategy of the electro-chemical analyses [33-43].

Since nano-materials enjoy very acceptable features, researchers have largely considered them. Moreover, nano-particles (NPs) may function as the conduction centers simplifying the electron transfer and providing larger catalytic surface area. Researchers have also presented diverse nanomaterials to modify the surface of electrodes and ameliorate their electro-chemical features [44-51].

In addition, experts in the field have been considerably attracted by the transition metal oxides because of their manifold features like thermal durability, different optical and electrical features as well as mechanical strength that led to their extensive utilization in particular in sensing interfaces [52,53]. Amongst diverse metal oxides, researchers have commonly applied copper oxide (CuO) for sensors because of their innate catalytic and electronic characteristics. Furthermore, CuO nano-structure shows numerous morphologies using the controlled synthetic processes that may exhibit effective electron transfer in the small sizes [54,55].

In the present work, a simplified, sensitive as well as precise electroanalytical procedure to determine methionine has been shown to be possible by utilizing synthesized CuO NFs modified GCE. The CuO NFs/GCE exhibit greater electrocatalytic activity, wide linear range and high sensitivity for determination of methionine over unmodified GCE. The CuO NFs/GCE was successfully employed for sensitive detection of methionine in urine sample.

EXPERIMENTAL PHASE

Instruments and chemicals

An Autolab potentiostat/galvanostat (PGSTAT 302N, Eco Chemie, the Netherlands) was utilized to measure electrochemicals. A platinum wire as the auxiliary electrode, CuO NFs/GCE as the working electrode and an Ag/AgCl/KCl (3.0 M) as reference electrode were used for electrochemical measurements. The ortho-phosphoric acid as well as the respective salts (KH2PO4, K2HPO4, K3PO4) with a pH ranging between 2.0 and 9.0 were utilized to procure buffer solution. The pH values were measured using a pH-meter (Metrohm 692 model, Herisau, Switzerland). Methionine and all other reagents were of the analytical grade, and they were obtained from Merck (Darmstadt, Germany). The phosphate buffer solution (PBS) was produced from concentrate phosphoric acid and its salts.

Preparation of electrode

The GCE was modified with CuO NF using a simple drop-casting method. To prepare the CuO NF stock solution in 1 mL of aqueous solution, the CuO NF (1 mg) was distributed by 30-minute ultrasonication. After that, a 5 μL CuO NF suspension was dropped on the screen-printed working electrode surface.

Then, the solvent was evaporated at an ambient temperature.

RESULTS AND DISCUSSION

Electrochemical behaviours of methionine on the various surface of electrodes

For studying electrochemical behaviours of methionine based on pH, providing an optimized pH-value could be of high significance to obtain acceptable outputs. Hence, the modified electrode was used for running experimentations under different pH amount ranging from 2.0 to 9.0. In the last step, the most promising outputs were seen in the case of electrooxidation of methionine at the pH equal to 7.0.

Figure 1 depicts CVs for methionine oxidation, at bare GCE (a), and CuO NFs/GCE (b) in 0.1 M PBS (pH of 7.0) solution containing 100.0 µM methionine at scan rate of 50 mV s-1. The anodic peak potential for methionine oxidation on the bare GCE was about 1280 mV, while on the CuO NFs/GCE, the peak potential was around 1000 mV. This reduction of around 280 mV proposes that the CuO NFs possesses highly efficient electrocatalytic activity considering the oxidation of methionine.

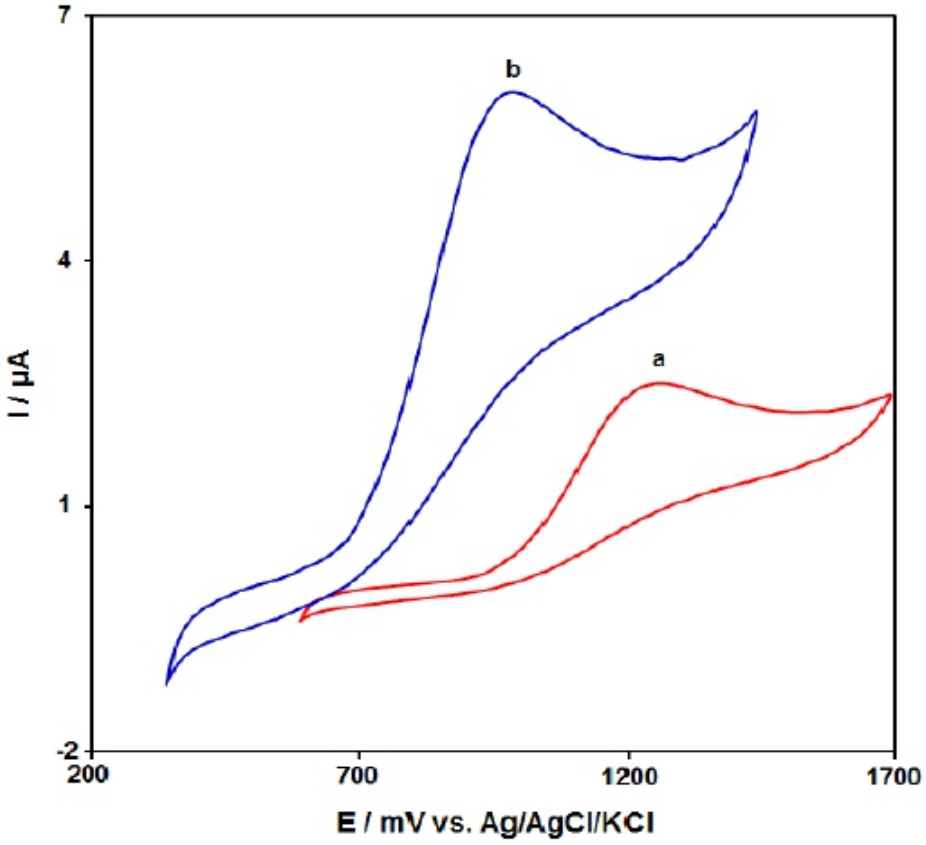

FIGURE 1 CVs of (a) bare GCE and (b) CuO NFs/GCE in the presence of 100.0 µM methionine. Scan rate was 50 mVs^{-1}

EFFECT OF SCAN RATE ON THE RESULTS

The relationship among scan rate and peak current presented promising data with respect to electrochemical mechanisms. Hence, the influence of scan rate onto the peak current of methionine was studied by LSV in the range of 10 to 400 mVs-1 in PBS (0.1 M, pH equal to 7.0) (Figure 2). The electrode response of methionine was a diffusion-controlled process since the peak current of oxidation was proportional to the square root of the scan rate (Figure 2, inset).

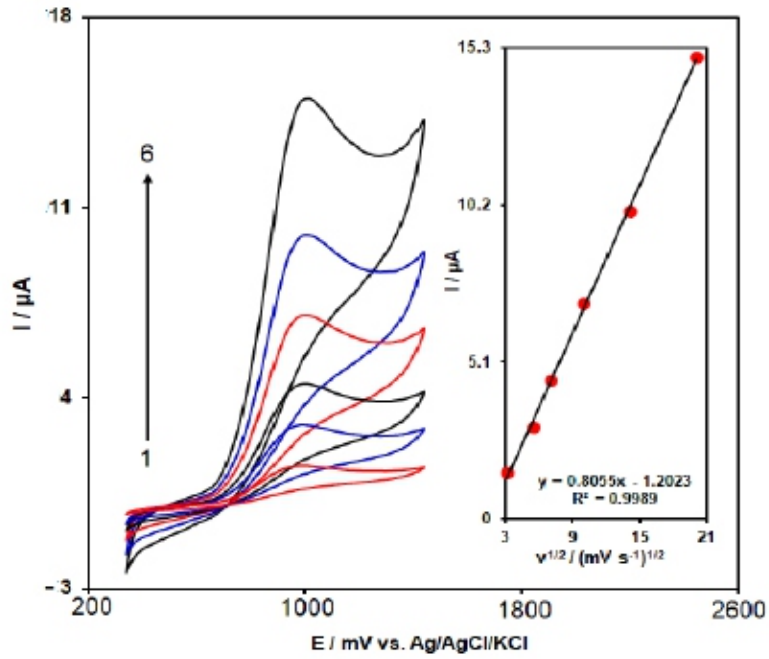

FIGURE 2 CVs of CuO NFs/GCE in 50.0 µM of methionine at different scan rates; (10, 30, 50, 100, 200 and 400 mV s^{-1}). Inset: Variation in the peak current vs. $v^{1/2}$

Chronoamperometric analyse

Chronoamperometric study was used for calculating the diffusion coefficient (D) of methionine on the surface CuO NFs/GCE at an optimum condition. Figure 3 displays chronoamperometric results of diverse concentrations of the methionine sample in PBS considering pH of 7.0. In addition, Cottrell equation is proposed in the case of the chronoamperometric analyses of electroactive moiety on the basis of the mass transfer restricted states [56]: Hence, D mean value equaled to 2.0×10^{-5} cm^2/s.

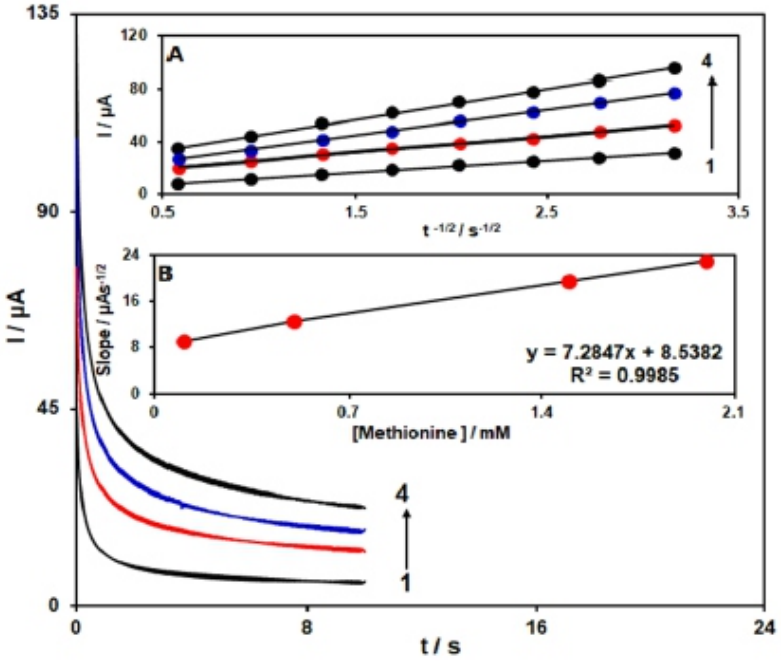

FIGURE 3 Chronoamperograms of CuO NFs/GCE in different concentration of methionine. (0.1, 0.5, 1.5 and 2.0 mM) Insets: (A) Plots of I vs. t -1/2. (B) Plot of the slope against methionine concentration

Calibration plot and detection limit

In this step, DPV was applied for determining methionine content with different concentration gradients at a pH of 7.0 (Figure 4). It was found that the peak currents of methionine oxidation at CuO NFs/GCE surface linearly depended on methionine concentrations above the range of 1.0–300.0 µM. The linear equation was as follows: y=0.0588x+0.2534, and the correlation coefficient was 0.9995. Also, the detection limit, Cm, of methionine was obtained using the following equation:

$$C_m=3s_b/m$$

The detection limit was 0.3 µM.

Analysis of real samples

Finally, the performance of CuO NFs/GCE as a new electrochemical sensor for analyzing of methionine in different samples of urine was evaluated. Table 1 shows obtained data as well as the recovery data proved the ability CuO NFs/GCE as a sensitive sensor in the case of the analysis of methionine in real samples.

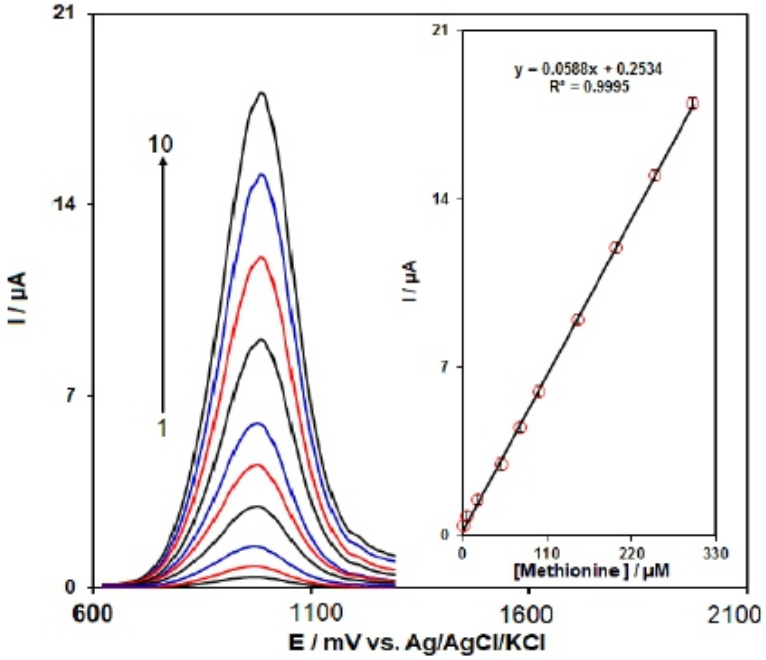

FIGURE 4 DPVs of CuO NFs/GCE in different concentrations of methionine (1.0, 5.0, 20.0, 50.0, 75.0, 100.0, 150.0, 200.0, 250.0 and 300.0 µM). Inset: plot of the peak current vs. methionine concentration

Table 1. The application of CuO NFs/GCE for the determination of methionine in urine (n=5)

Spiked(µM)	Found (µM)	Recovery (%)	R.S.D. (%)
0	-	-	-
7.0	6.9	98.6	3.2
12.0	12.2	101.7	1.8
17.0	16.9	99.4	2.9
22.0	22.5	102.3	2.4

CONCLUSION

This research provided one of the effective affordable analytical procedure for sensing methionine in PBS with the use of a CuO NFs modified GCE. The results indicated the greater surface area of electrode

by the presence of CuO NFs that led to the effective interface for electrochemical reaction of methionine. By DPV, the proposed modified electrode linearly responded in the broad ranges from 1.0-300.0 μM with the LOD equal to 0.3 μM. Also, the results showed CuO NFs/GCE sensitivity to determine methionine in urine samples with reasonable accuracy, which reflected the possible utilization of this technique to detecting methionine in real samples.

Orcid:

Hadi Beitollahi: https://orcid.org/0000-0002-0669-5216

REFERENCES

[1] N. Tavakkoli, N. Soltani, E. Khorshidi, RSC Adv., 2017, 7, 21827-21836.
[2] A. Salimi, M. Roushani, Electroanalysis, 2006, 18, 2129-2136.
[3] A. DiRocco, M. Tagliati, D. Dorfman, J. Moise, D. Simpson, Neurology, 1996, 46, 6124.
[4] S. Toyokuni, K. Okamoto, J. Yodoi, H. Hiai, FEBS Lett., 1995, 358, 1-3.
[5] P. Jandik, J. Cheng, J. Evrovski, N. Avdalovic, J. Chromatogr. B: Biomed. Sci. Appl., 2001, 759, 145-151.
[6] A. Zinellu, S. Sotgia, M.F. Usai, E. Zinellu, A.M. Posadino, L. Gaspa, R. Chessa, A. Pinna, F. Carta, L. Deiana, Anal. Biochem., 2007, 363, 91-96.
[7] S.P. Stabler, P.D. Marcell, E. R. Podell, R. H. Allen, Anal. Biochem., 1987, 162, 185-196
[8] D.R. Murphy-Chutorian, M.P. Wexman, A.J. Grieco, J.A. Heininger, E. Glassman, G.E. Gaull, S.K. Ng, F. Feit, K. Wexman, A.C. Fox, J. Am. Coll. Cardiol., 1985, 6, 725-730.
[9] S.H. Mudd, N. Braverman, M. Pomper, K. Tezcan, J. Kronick, P. Jayakar, C. Garganta, M.G. Ampola, H.L. Levy , S.E. McCandless, Mol. Genet. Metab., 2003, 79, 6-16.
[10] Z. Deáková, Z. Ďuračková, D.W. Armstrong, J. Lehotay, J. Chromatogr. A, 2015, 1408, 118-124.
[11] L. Kuang, L. Zhang, A.Z. Xu, Z.M. Li, R.P. Liang, J.D. Qiu, Sens. Actuators B: Chem., 2017, 244, 1031-1036.
[12] P.C. Huang, N. Gao, J.F. Li, F.Y. Wu, Sens. Actuators B: Chem., 2018, 255, 2779-2784.
[13] M. Kameya, M. Himi, Y. Asano, Anal. Biochem., 2014, 447, 33-38.
[14] Y. Li, S. Mei, S. Liu, X. Hun, J. Pharm. Biomed. Anal., 2019, 165, 94-100.
[15] Y. Shinohara, H. Hasegawa, K. Tagoku, T. Hashimoto, J. chromatogr. B: Biomed. Sci. Appl., 2001,758, 283-288.
[16] H.M.A. Hasan, I.H. Habib, A.M. Ali, Eur. Chem. Bull., 2017, 6, 355-358.
[17] N.A. Odewunmi, A.N. Kawde, M. Ibrahim, Sens. Actuators B: Chem., 2019, 281,765-773.
[18] L. Agüı, J. Manso, P. Yáñez-Sedeño, J. Pingarrón, Talanta, 2004, 64, 1041-1047.
[19] F. Chekin, S. Bagheri, S.B.A. Hamid, Sens. Actuators B: Chem., 2013, 177, 898-903.
[20] H. Beitollahi, S. Tajik, F. Garkani-Nejad, M. Safaei, J. Mater. Chem. B, 2020, 8, 5826-5844.
[21] A.J. Jeevagan, S.A. John, Bioelectrochemistry, 2012, 85, 50-55.
[22] H. Karimi-Maleh, F. Karimi, M. Alizadeh, A. L. Sanati, Chem. Rec. 2020, 20, 682-692.
[23] N. Rabiee, M. Safarkhani, M. Rabiee, Asian J. Nanosci. Mater., 2018, 1, 63-73.
[24] H. Beitollahi, F. Garkani-Nejad, S. Tajik, M. R. Ganjali, Iran. J. Pharm. Res., 2019, 18, 80.
[25] M. Bijad, H. Karimi-Maleh, M.A. Khalilzadeh, Food Anal. Methods, 2013, 6, 1639-1647.
[26] P. Prasad, N.Y. Sreedhar, Chem. Methodol., 2018, 2, 277-290.
[27] N.B. Messaoud, M.E. Ghica, C. Dridi, M.B. Ali, C.M. Brett, Sens. Actuators B: Chem., 2017, 253, 513-522.
[28] J. Ghodsi, A.A. Rafati, Y. Shoja, Adv. J. Chem. A, 2018, 1, 39-55.
[29] H. Beitollahi, H. Mahmoudi-Moghaddam, S. Tajik, Anal. Lett., 2019, 5, 1432-1444.
[30] J. V. Piovesan, E.R. Santana, A. Spinelli, J. Electroanal. Chem., 2018, 813, 163-170.
[31] F. Tahernejad-Javazmi, M. Shabani-Nooshabadi, H. Karimi-Maleh, Talanta, 2018, 176, 208-213.
[32] W. Liu, Q. Shi, G. Zheng, J. Zhou, M. Chen, Anal. Chim. Acta, 2019, 1075, 81-90.
[33] M. Rizwan, M. Hazmi, S.A. Lim, M.U. Ahmed, J. Electroanal. Chem., 2019, 833, 462-470.
[34] M.R. Ganjali, H. Beitollahi, R. Zaimbashi, S. Tajik, M. Rezapour, B. Larijani, Int. J. Electrochem. Sci., 2018, 13, 2519-2529.
[35] S. Alavi-Tabari, M.A. Khalilzadeh, H. Karimi-Maleh, J. Electroanal. Chem., 2018, 811, 84-88.
[36] A. Özcan, D. Topçuoğulları, A.A. Özcan, Sens. Actuators B: Chem., 2019, 284, 179-185.
[37] M.R. Ganjali, Z. Dourandish, H. Beitollahi, S. Tajik, L. Hajiaghababaei, B. Larijani, Int. J. Electrochem. Sci., 2018, 13, 2448-2461.

[38] A. Baghizadeh, H. Karimi-Maleh, Z. Khoshnama, A. Hassankhani, M. Abbasghorbani, Food Anal. Methods, 2015, 8, 549-557.
[39] S. Mohammadi, A. Taheri, Z. Rezayati-Zad, Prog. Chem. Biochem. Res., 2018 , 1, 1-10.
[40] H. Beitollahi, F. Garkani-Nejad, S. Tajik, Sh. Jahani, P. Biparva, Int. J. Nano Dimens, 2017, 8, 197-205.
[41] W.H. Elobeid, A.A .Elbashir, Prog. Chem. Biochem. Res., 2019, 2, 24-33.
[42] S. Tajik, M.A. Taher, H. Beitollahi, Ionics, 2014, 20, 1155-1161.
[43] M. Miraki, H. Karimi-Maleh, M.A. Taher, S. Cheraghi, F. Karimi, S. Agarwal, V.K. Gupta, J. Mol. Liq., 2019, 278, 672-676.
[44] D. Perevezentseva, K. Skirdin, E. Gorchakov, V. Bimatov, Key Eng. Mater., 2016, 685, 563-568.
[45] H. Karimi-Maleh, K. Cellat, K. Arıkan, A. Savk, F. Karimi, F. Şen, Mater. Chem. Phys., 2020, 250, 123042.
[46] M.M. Motaghi, H. Beitollahi, S. Tajik, R. Hosseinzadeh, Int. J. Electrochem. Sci., 2016, 11, 7849-7860.
[47] H. Karimi-Maleh, F. Karimi, Y. Orooji, Gh. Mansouri, A. Razmjou, A. Aygun, F. Sen, Sci. Rep., 2020, 10, 11699.
[48] G. Vinodhkumar, R. Ramya, M. Vimalan, I. Potheher, A. Cyrac Peter, Prog. Chem. Biochem. Res., 2018, 1, 40-49.
[49] H. Beitollahi, Z. Dourandish, S. Tajik, M.R. Ganjali, P. Norouzi, F. Faridbod, J. Rare Earth., 2018, 36, 750-757.
[50] H. Karimi-Maleh, F. Karimi, S. Malekmohammadi, N. Zakariae, R. Esmaeili, S. Rostamnia, M.L. Yola, N. Atar, Sh. Movagharnezhad, S. Rajendran, A. Razmjou, Y. Orooji, S. Agarwal, V.K. Gupta, J. Mol. Liq., 2020, 310, 113185.
[51] H. Mahmoudi-Moghaddam, S. Tajik, H. Beitollahi, Microchem. J., 2019, 150, 104085.
[52] P. Bollella, G. Fusco, C. Tortolini, G. Sanzo`, G. Favero, L. Gorton , R. Antiochia, Biosens. Bioelectron., 2017, 89, 152–166.
[53] H. Karimi-Maleh, M. Sheikhshoaie, I. Sheikhshoaie, M. Ranjbar, J. Alizadeh, N.W. Maxakato, A. Abbaspourrad, New J. Chem., 2019, 43, 2362-2367.
[54] B. Mahmoud, M. Khairy, F. Rashwan, C. Fosterb, C. Banks, RSC Adv., 2016, 6, 14474–14482.
[55] Y. Wang, D. Fan, D. Wu, Y. Zhang, H. Ma, B. Du , Q. Wei, Sens. Actuators B: Chem., 2016, 236, 241–248.
[56] A. J. Bard, L.R. Faulkner, Electrochemical Methods Fundamentals and Applications, 2nd ed. Wiley, New York, 2001.

How to cite this article:

Maryam Ebrahimi, Hadi Beitollahi*.
CuO nanoflowers modified glassy carbon electrode for the electrochemical determination of methionine. Eurasian Chemical Communications, 2021, 3(1), 19-25. Link: http://www.echemcom.com /article_120300.html

Sensitive Detection of Hydrochlorothiazide using Ce^{3+}/NiO Hexagonal Nanoparticles Modified Glassy Carbon Electrode

Sajedeh Salari[a], Hadi Beitollahi[b,*]

[a]Department of Chemistry, Graduate University of Advanced Technology, Kerman, Iran

[b]Environment Department, Institute of Science and High Technology and Environmental Sciences, Graduate University of Advanced Technology, Kerman, Iran

*Corresponding Author: Email - h.beitollahi@yahoo.com, Tel.: +983426226613

ABSTRACT

The present research presented a novel modification approach for modifying a glassy carbon electrode on the basis of the Ce3+/NiO hexagonal nanoparticles (Ce^{3+}/NiO hexagonal NPs/GCE). In so doing, we devised the new modified electrode for using as one of the sensitive sensors for detecting the trace amounts of hydrochlorothiazide. Moreover, it is an acceptable electrocatalyst for catalytic oxidation of hydrochlorothiazide by shifting the overpotential toward less positive potential and enhancing catalytic current in comparison to the bare GCE. In a concentration range 0.1 to 700.0 μM in a phosphate buffer solution (PBS) at a pH of 7.0, the responses were linear and hydrochlorothiazide detection limit for this method was 0.03 μM (S/N=3). Furthermore, this sensor successfully detected hydrochlorothiazide in hydrochlorothiazide tablets and urine samples with satisfactory recovery ranges, indicating a promising application in biological samples, pharmaceutical compounds analysis and clinical diagnosis.

KEYWORDS : Electrochemical sensors; nanochemistry; voltammetry.

INTRODUCTION

Hypertension is another name for high blood pressure. The prolonged increased blood pressure has been identified as one of the main risk factors for stroke, kidney failure and heart attacks [1,2]. These problems may be less likely to occur if blood pressure is controlled. Therefore, the first-line medication for hyper-tension contains thiazide-diuretics, angiotensin converting enzyme inhibitors, angiotensin receptor blocker as well as calcium channel blockers [3].

Researchers consider hydro-chlorothiazide (i.e., 6-chloro-3,4-dihydro-2H-1,2,4-benzothiadiazine-7-sulfonamide 1,1-dioxide) as one of the thiazide diuretics [4]. Hydrochlorothiazide has been proposed as one of the drugs with the widespread utilizations worldwide to treat the high blood pressure since the advent of chlorothiazide in 1957. Hydrochlorothiazide functions on the kidney and inhibits sodium and chloride ions re-absorption into the nephron-contoured tubules. Moreover, it prevents water re-absorption and decreases the blood pressure. Additionally, hydrochlorothiazide has uses in curing the renal tubular acidosis, edema, diabetes insipiddus and preventing the kidney stone [5,6]. Notably, half-life of hydrochlorothiazide is variable from 6-15 h and approximately 50% to 60% of the oral administration of the drug excreted via urine [7]. An over-dose of hydrochlorothiazide of the patients' loss fluid and electrolyte and the reported symptoms have been dizziness, sedation or impaired consciousness, hypo-tension as well as cramps in the muscles [8]. Hence, the determination of hydrochlorothiazide in human fluids and pharmaceutical compounds is very important.

Numerous methods have been designed to detect hydrochlorothiazide, including HPLC [9], liquid chromatography tandem mass spectrometry [10], ultraviolet spectrophotometry [11], and

electrochemistry [12]. Although such methods are sensitive, there are restrictions such as high costs and complex analysis processes which are cumbersome for analysis. In contrast, electrochemical methods have become prominent in analyte detection because of their low cost, rapid response time, high sensitivity, simplicity and selectivity [13-24].

According to the studies, electro-chemical procedures with the use of the chemically modified electrodes (CMEs) have a widespread utilization as the selective and sensitive analytical techniques to determine trace amount of electroactive prominent compounds [25-35]. However, a major feature of CMEs is their capability of catalyzing the electrode procedure through considerable decline in the over-potential on the basis of the un-modified electrodes. Consequently, choosing materials for constructing diverse modified electrodes to detectanalyte is of high importance.

Recently, nanomaterials have been widely used as modifier in electrochemical detection due to their very good electrical conductivity, larger surface areas [36-43]. In addition, nickel oxide (NiO) that is one of the p-type semiconductors with the broad band gap equal to 3.7 eV in the room temperature and the increased isoelectric point (IEP) of ~10.7, is of particular interest in the environmental, energy as well as biological researches because of their effective electro-catalytic features, acceptable oxygen-ion conductivity, non-toxicity, bio-compatibility, specific capacity equal to 2785 Fg^{-1} and porosity features [44-49]. Nevertheless, for electrochemical applications, the increased conductivity has been proposed as one of the prime parameters for improving its electrochemical functions. Therefore, for improvements in the electrical features of metal oxides, researchers typically run heteroatom doping. Conventionally, metallic dopants have entered the lattice of metal oxides for elevating its electrocatalytic behaviors [50]. As an instance, in the published investigations, some researches confirmed doping heteroatoms like Li^{+}, La^{3+}, Co^{3+} as well as Y^{3+} for improving its electro catalytic behaviors for diverse utilizations [51-54]. Herein, we used rare earth ions (Ce^{3+}) doping to improve the electrocatalytic performance of NiO nanostructures.

The present work aimed at employing the electrochemical method for determination of hydrochlorothiazide at the synthesized Ce^{3+}/NiO hexagonal NPs modified GCE. An excellent electrocatalytic activity was observed regarding hydrochlorothiazide oxidation with the increased oxidation peak current and decrease of overpotential. Also, using this developed sensor, the determination of hydrochlorothiazide was carried out in tablets and urine samples.

EXPERIMENTAL SECTION

Instruments and chemicals

An Autolab potentiostat/galvanostat (PGSTAT 302N, Eco Chemie, the Netherlands) was utilized to measure electrochemicals. A platinum wire as the auxiliary electrode, CuO NFs/GCE as the working electrode and an Ag/AgCl/KCl (3.0 M) as reference electrode were used for electrochemical measurements. The ortho-phosphoric acid as well as the respective salts (KH_2PO_4, K_2HPO_4, K_3PO_4) with a pH ranging between 2.0 and 9.0 were utilized to procure buffer solution. The pH values were measured using a pH-meter (Metrohm 692 model, Herisau, Switzerland).

Hydrochlorothiazide and all other reagents were of the analytical grade, and were obtained from Merck (Darmstadt, Germany). The phosphate buffer solution (PBS) was produced from concentrate phosphoric acid and its salts.

Preparation of electrode

The GCE was modified with Ce^{3+}/NiO hexagonal NPs using a simple drop-casting method. To prepare the CuO NF stock solution in 1 mL of aqueous solution, the Ce^{3+}/NiO hexagonal NPs (1 mg) was distributed by 30-minute ultrasonication. After that, a 5 µL Ce^{3+}/NiO hexagonal NPs suspension was dropped on the glassy carbon working electrode surface. Then, the solvent was evaporated at an ambient temperature. The surface areas of the Ce^{3+}/NiO hexagonal NPs/GCE and the bare GCE were obtained by CV using 1mM $K_3Fe(CN)^6$ at different scan rates. Using Randles-Sevcik formula [55] in Ce^{3+}/NiO hexagonal NPs/GCE, the electrode surface was found 0.156 cm2 which was about 4.96 times greater than bare GCE.

RESULTS AND DISCUSSION

Electrochemical behaviours of hydrochlorothiazide on the various surface of electrodes

For studying electrochemical behaviours of hydrochlorothiazide based on pH, providing an optimized pH-value could be of high significance to obtain acceptable outputs. Hence, the modified electrode was used for running experimentations under different pH amount ranging from 2.0 to 9.0 (Figure 1). In the last step, the most promising results were seen in the case of electrooxidation of hydrochlorothiazide at the pH equal to 7.0.

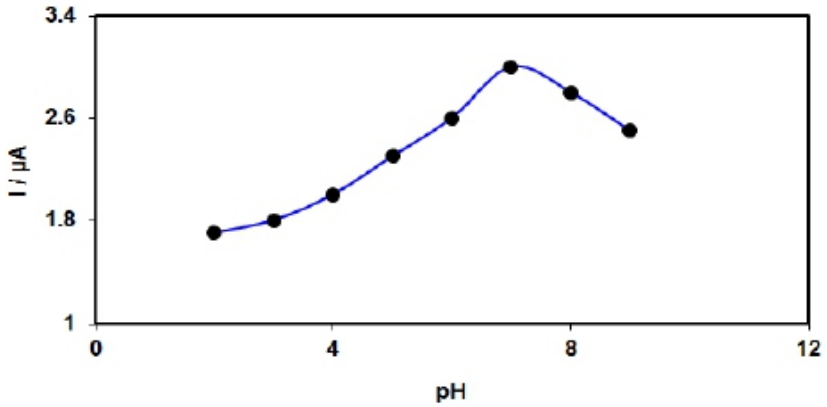

FIGURE 1 Plot of Ip vs. pH obtained from DPVs of Ce^{3+}/NiO hexagonal NPs/GCE in a solution containing 100.0 µM of hydrochlorothiazide in 0.1 PBS with different pHs (2.0, 3.0, 4.0, 5.0, 6.0, 7.0, 8.0 and 9.0)

Figure 2 depicts CVs for hydrochlorothiazide oxidation, at bare GCE (a), and Ce^{3+}/NiO hexagonal NPs/GCE (b) in 0.1 M PBS (pH of 7.0) solution containing 100.0 µM hydrochlorothiazide at scan rate of 50 mV s^{-1}. The anodic peak potential for hydrochlorothiazide oxidation on the bare GCE was about 1150 mV, while on the Ce^{3+}/NiO hexagonal NPs/GCE, the peak potential was around 800 mV. This reduction of around 350 mV proposes that the Ce^{3+}/NiO hexagonal NPs possesses highly efficient electrocatalytic activity considering the oxidation of hydrochlorothiazide.

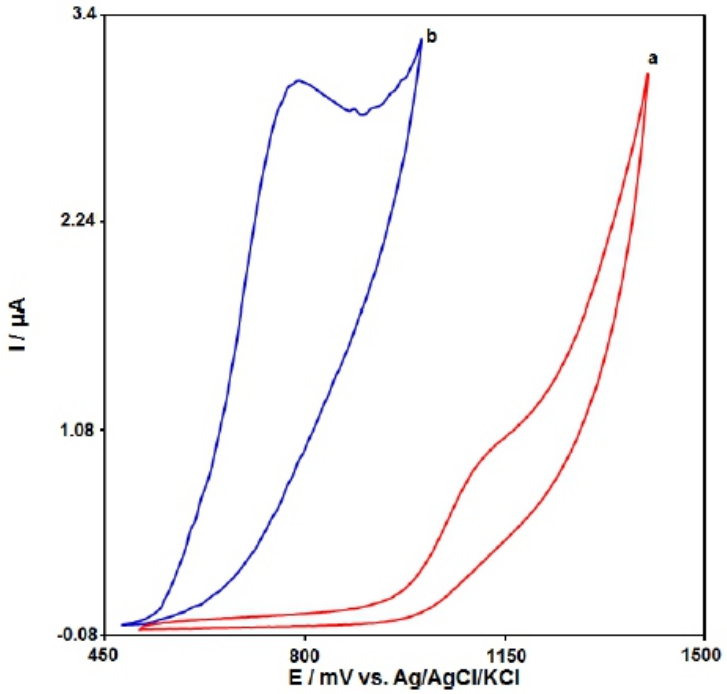

FIGURE 2 CVs of (a) bare GCE and (b) CuO NFs/GCE in the presence of 100.0 µM hydrochlorothiazide. Scan rate was 50 mVs^{-1}

Effect of scan rate on the results

The relationship between scan rate and peak current shows promising data with respect to electrochemical mechanisms. Hence, the influence of scan rate onto the peak current of hydrochlorothiazide was studied by LSV (Figure 3). The electrode response of hydrochlorothiazide was a diffusion-controlled process since the peak current of oxidation was proportional to the square root of the scan rate (Figure 3, inset).

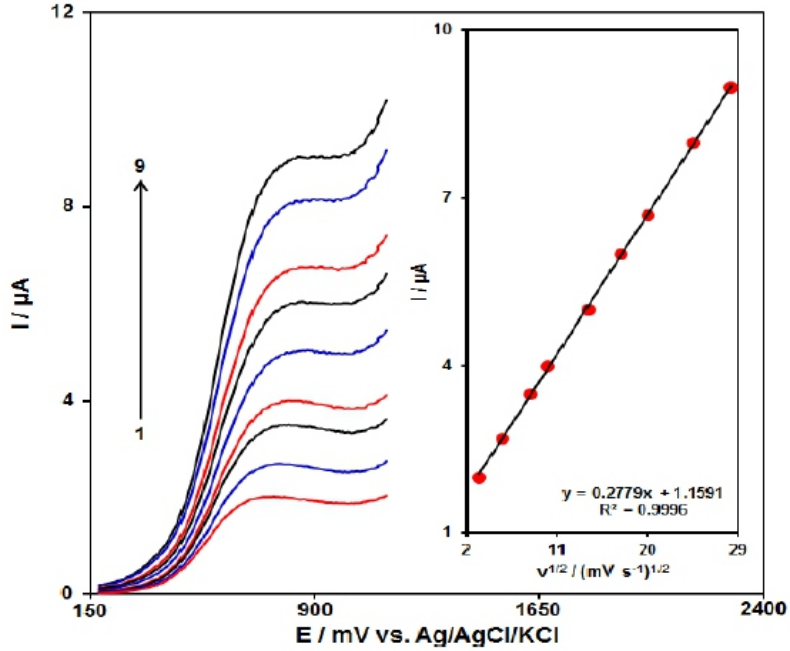

FIGURE 3 CVs of Ce^{3+}/NiO hexagonal NPs/GCE in 100.0 µM of hydrochlorothiazide at different scan rates; (10, 30, 70, 100, 200, 300, 400, 600 and 800 mV s^{-1}). Inset: Variation in the peak current vs. $v^{1/2}$

Chronoamperometric analyse

Chronoamperometric study was used to calculate the diffusion coefficient (D) of methionine on the surface Ce^{3+}/NiO hexagonal NPs/GCE at an optimum condition. Figure 4 displays chronoamperometric results of diverse concentrations of the hydrochlorothiazide sample in PBS considering pH of 7.0. In addition, Cottrell equation is proposed in the case of the chronoamperometric analyses of electroactive moiety in the basis of the mass transfer restricted states [55]. Hence, D mean value equaled to 2.4×10^{-5} $cm^2 s^{-1}$.

Calibration plot and detection limit

In this step, DPV was applied for determining hydrochlorothiazide content with different concentration gradients at a pH of 7.0 (Figure 5). (Step potential=0.01 V and pulse amplitude=0.025 V). It was found that the peak currents of hydrochlorothiazide oxidation at Ce^{3+}/NiO hexagonal NPs/GCE surface linearly depended on hydrochlorothiazide concentrations above the range of 0.1–700.0 µM. The detection limit was 0.03 µM. The comparison of the results for the detection of hydrochlorothiazide with different modified electrodes in the literatures are listed in Table 1.

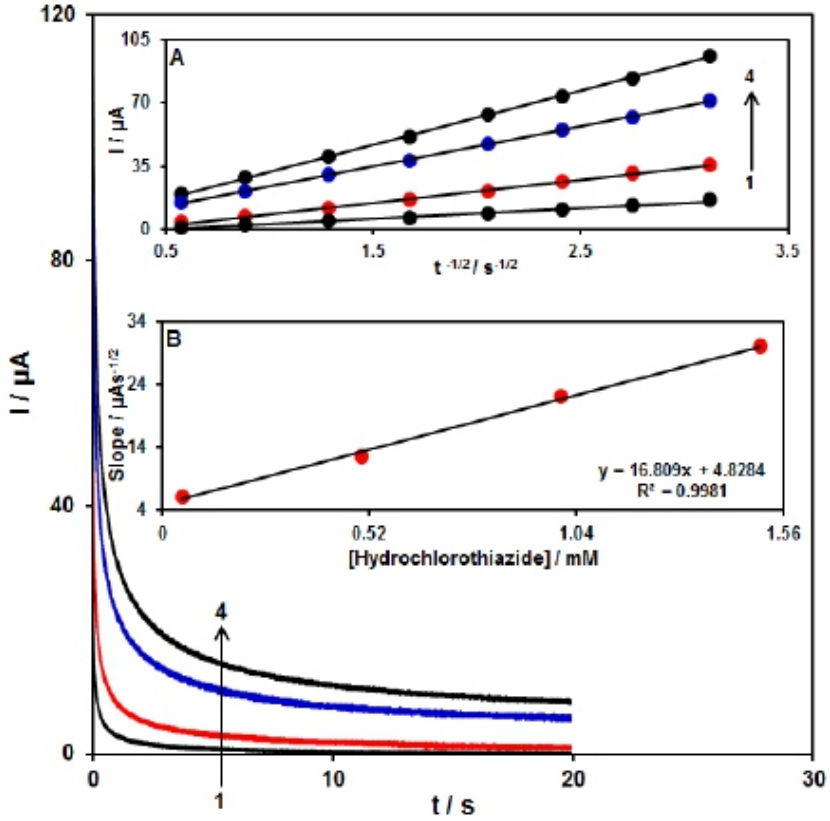

FIGURE 4 Chronoamperograms of Ce^{3+}/NiO hexagonal NPs/GCE in different concentration of hydrochlorothiazide. (0.05, 0.5, 1.0 and 1.5mM) Insets: (A) Plots of I vs. $t^{-1/2}$. (B) Plot of the slope against methionineconcentration

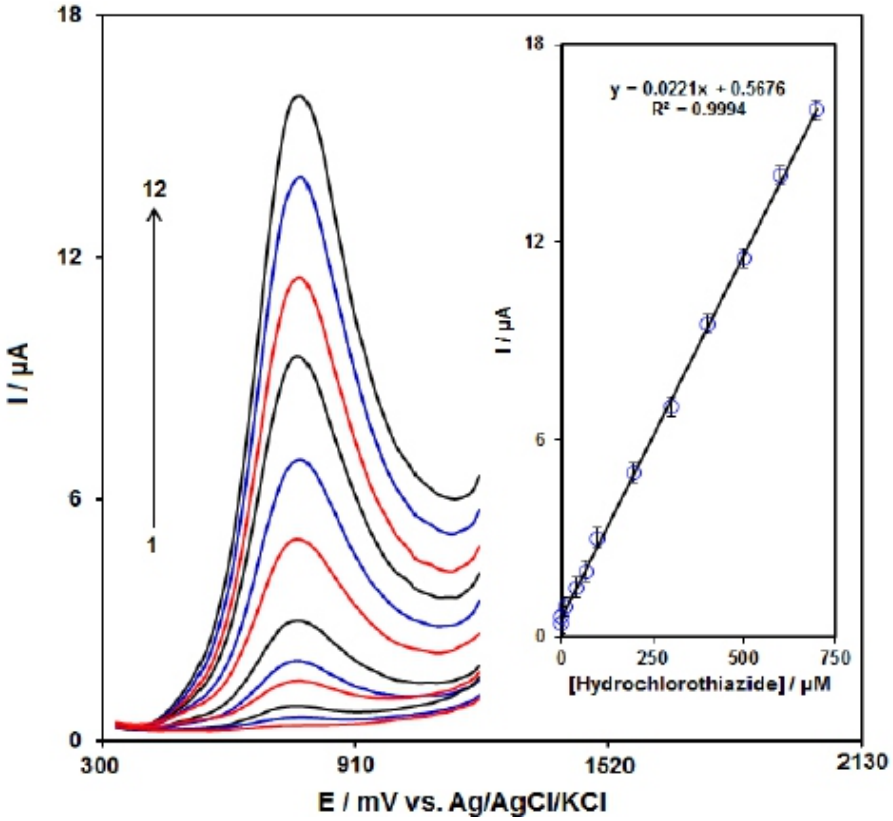

FIGURE 5 DPVs of Ce^{3+}/NiO hexagonal NPs/GCE in different concentrations of hydrochlorothiazide (0.1, 1.0, 10.0, 40.0, 70.0, 100.0, 200.0, 300.0, 400.0, 500.0, 600.0 and 700.0 µM). Inset: plot of the peak current vs. hydrochlorothiazide concentration

TABLE 1 Comparing performance of purposed electrochemical sensor with others for detection of hydrochlorothiazide

Ref.	Limit of Detection (µM)	Linear Range (µM)	Method	Electrochemical Sensor
[56]	21.2 µmol dm^{-3}	0.22–5.82 mmol dm^{-3}	Amperometry	Nickel Nanowrinkles/Carbon Paste Electrode
[57]	2.71 nM	0.01-0.2 µM	Square Wave Voltammetry	Graphene Oxide/GCE
[58]	2.8×10^{-8} M	1.0×10^{-7}-2.0 $\times10^{-5}$ M	Adsorptive stripping voltammetry	Multi-Walled Carbon Nanotube/GCE
[59]	0.14 µM	1.0–500.0 µM	Square Wave Voltammetry	NiO NPs-Benzoylferrocene/Carbon Paste Electrode
[60]	8.55 µM	28.5-300.0 µM	DPV	Poly L-Glutamic Acid/ Screen-Printed Carbon Electrode
This Work	0.03 µM	0.1-700.0 µM	DPV	Ce^{3+}/NiO Hexagonal NPs/GCE

Analysis of real samples

Finally, the performance of Ce^{3+}/NiO hexagonal NPs/GCE as a new electrochemical sensor for analyzing of hydrochlorothiazide in hydrochlorothiazide tablets and urine samples was evaluated. Table 2 shows obtained data as well as the recovery data proving the ability of Ce^{3+}/NiO hexagonal NPs/GCE as a sensitive sensor in the case of the analysis of hydrochlorothiazide in real samples.

TABLE 2 The application of Ce^{3+}/NiO hexagonal NPs/GCE for determination of hydrochlorothiazide in hydrochlorothiazide tablets and urine samples (n=5)

(%)R.S.D.	Recovery (%)	Found (μM)	Spiked (μM)	Sample
3.2	-	3.0	0	Hydrochlorothiazide Tablets
1.9	98.7	7.9	5.0	
2.8	103.1	13.4	10.0	
2.3	97.2	17.5	15.0	
2.1	100.8	23.2	20.0	
-	-	-	0	Urine
1.9	102.9	7.2	7.0	
2.8	98.3	11.8	12.0	
3.0	102.3	17.4	17.0	
3.1	97.7	21.5	22.0	

CONCLUSION

This research demonstrated the fabrication of Ce^{3+}/NiO hexagonal NPs/GCE and the respective utilization to determine hydrochlorothiazide. The results showed catalysis of hydrochlorothiazide oxidation at a pH of 7.0 and the respective peak potential switched to a less positive potential at the surface of the modified electrode. Finally, this developed sensor can be successfully utilized to analyze hydrochlorothiazide in hydrochlorothiazide tablets and the urine sample. Hence, the sensor can be helpful with the acceptable analytical advancements.

Orcid:

Hadi Beitollahi: https://orcid.org/0000-0002-0669-5216

REFERENCES

[1] S. Ahmed, N.N. Atia, N.A. Mohamed, Talanta, 2011, 84, 666–672.
[2] D.T. Gimenes, M.C. Marra, J.M. de-Freitas, R.A. Abarza-Munoz, E.M. Richter, Sens. Actuators B: Chem., 2015, 212, 411-418.
[3] P.A. James, S. Oparil, B.L. Carter, W.C. Cushman, C. Dennison-Himmelfarb, J. Handler, D.T. Lackland, M.L. LeFevre, T.D. MacKenzie, O. Ogedegbe, S.C. Smith, L.P. Svetkey, S.J. Taler, R.R. Townsend, J.T. Wright, A.S. Narva, E. Ortiz, JAMA, 2014, 311, 507-520.
[4] H. Beitollahi, F. Ebadi-Nejad, F. Shojaie, M. Torkzadeh-Mahani, Anal. Methods, 2016, 8, 6185-6193.
[5] J.A. Schoenberger, J. Hypertens. Suppl., 1995, 13, S43–S47.
[6] L.E. Ramsay, W.W. Yeo, J. Hypertens. Suppl., 1995, 13, S73–S76.

[7] N. Kumar, R.N. Goyal, J. Electrochem. Soc., 2017, 164, B240.
[8] C.A.R. Salamanca-Neto, A.P.P. Eisele, V.G. Resta, J. Scremin, E.R. Sartori, Sens. Actuators B: Chem., 2016, 230, 630-638.
[9] M.M. Ayad, M.M. Hosny, A.E. Ibrahim, O. M. El-Abassy, F.F. Belal, J. Iran. Chem. Soc., 2020, 17, 1725–1730.
[10] E.F. Elkady, A.A. Mandour, F.K. Algethami, A.A. Aboelwafa, F. Farouk, Microchem. J., 2020, 155, 104757.
[11] H. Syahputra, M.S.A. Muchlisyam, M. A. Masfria, Asian J. Pharm. Res. Develop., 2019, 7, 1-4.
[12] H.T. Purushothama, Y.A. Nayaka, Chem. Phys. Lett., 2019, 734, 136718.
[13] H. Karimi-Maleh, F. Karimi, M. Alizadeh, A. L. Sanati, Chem. Rec., 2020, 20, 682-692.
[14] A.J. Jeevagan, S.A. John, Bioelectrochemistry, 2012, 85, 50-55.
[15] T. Jiang, L.Qi, X. Lu, C. Hou, W. Qin, J. Electroanal. Chem., 2020, 878, 114562.
[16] H. Beitollahi, F. Garkani-Nejad, S. Tajik, M. R. Ganjali, Iran. J. Pharm. Res., 2019, 18, 80-90.
[17] H. Karimi-Maleh, M. Sheikhshoaie, I. Sheikhshoaie, M. Ranjbar, J. Alizadeh, N.W. Maxakato, A. Abbaspourrad, New J. Chem., 2019, 43, 2362-2367.
[18] T.T. Calam, Electroanalysis, 2020, 32, 149-158.
[19] H. Beitollahi, H. Mahmoudi-Moghaddam, S. Tajik, Anal. Lett., 2019, 5, 1432-1444.
[20] C. Raril, J.G. Manjunatha, Microchem. J., 2020, 154, 104575.
[21] S. Alavi-Tabari, M.A. Khalilzadeh, H. Karimi-Maleh, J. Electroanal. Chem., 2018, 811, 84-88.
[22] J.V. Piovesan, E.R. Santana, A. Spinelli, J. Electroanal. Chem., 2018, 813, 163-170.
[23] H. Beitollahi, S. Tajik, F. Garkani-Nejad, M. Safaei, 2020, J. Mater. Chem. B, 2020, 8, 5826-5844.
[24] B. Ibarlucea, A.P. Roig, D. Belyaev, L. Baraban, G. Cuniberti, Microchim. Acta, 2020, 187, 1-11.
[25] M. Rizwan, M. Hazmi, S.A. Lim, M.U. Ahmed, J. Electroanal. Chem., 2019, 833, 462-470.
[26] M.R. Ganjali, Z. Dourandish, H. Beitollahi, S. Tajik, L. Hajiaghababaei, B. Larijani, Int. J. Electrochem. Sci., 2018, 13, 2448-2461.
[27] F. Tahernejad-Javazmi, M. Shabani-Nooshabadi, H. Karimi-Maleh, Talanta, 2018, 176, 208-213.
[28] A. Özcan, D. Topçuoğulları, A. A. Özcan, Sens. Actuators B: Chem., 2019, 284, 179-185.
[29] H. Beitollahi, F. Garkani-Nejad, S. Tajik, Sh. Jahani, P. Biparva, Int. J. Nano Dimens, 2017, 8, 197-205.
[30] A. Baghizadeh, H. Karimi-Maleh, Z. Khoshnama, A. Hassankhani, M. Abbasghorbani, Food Anal. Methods, 2015, 8, 549-557.
[31] A.R. Marlinda, S. Sagadevan, N. Yusoff, A. Pandikumar, N.M. Huang, O. Akbarzadeh, M.R. Johan, J. Alloys Compd., 2020, 847, 156552.
[32] S. Tajik, M.A. Taher, H. Beitollahi, Ionics, 2014, 20, 1155-1161.
[33] L. Durai, S. Badhulika, Sens. Actuators B: Chem., 2020, 325, 128792.
[34] M.R. Ganjali, H. Beitollahi, R. Zaimbashi, S. Tajik, M. Rezapour, B. Larijani, Int. J. Electrochem. Sci., 2018, 13, 2519-2529.
[35] M. Bijad, H. Karimi-Maleh, M.A. Khalilzadeh, Food Anal. Methods, 2013, 6, 1639-1647.
[36] D. Perevezentseva, K. Skirdin, E. Gorchakov, V. Bimatov, Key Eng. Mater., 2016, 685, 563-568.
[37] M.M. Motaghi, H. Beitollahi, S. Tajik, R. Hosseinzadeh, Int. J. Electrochem. Sci., 2016, 11, 7849-7860.
[38] H. Karimi-Maleh, F. Karimi, Y. Orooji, Gh. Mansouri, A. Razmjou, A. Aygun, F. Sen, Sci. Rep., 2020, 10, 11699.
[39] S. Sahoo, P.K. Sahoo, S. Manna, A.K. Satpati, J. Electroanal. Chem., 2020, 876, 114504.
[40] H. Karimi-Maleh, F. Karimi, S. Malekmohammadi, N. Zakariae, R. Esmaeili, S. Rostamnia, M.L. Yola, N. Atar, Sh. Movagharnezhad, S. Rajendran, A. Razmjou, Y. Orooji, S. Agarwal, V.K. Gupta, J. Mol. Liq., 2020, 310, 113185.
[41] H. Beitollahi, Z. Dourandish, S. Tajik, M. R. Ganjali, P. Norouzi, F. Faridbod, J. Rare Earth., 2018, 36, 750-757.
[42] H. Karimi-Maleh, K. Cellat, K. Arıkan, A. Savk, F. Karimi, F. Şen, Mater. Chem. Phys., 2020, 250, 123042.
[43] H. Mahmoudi-Moghaddam, S. Tajik, H. Beitollahi, Microchem. J., 2019, 150, 104085.
[44] A. Salimi, E. Sharifi, A. Noorbakhash, S. Soltanian, Biosens. Bioelectron., 2007, 22, 3146–3153.
[45] A. Salimi, A. Noorbakhash, E. Sharifi, A. Semnani, Biosens. Bioelectron., 2008, 24, 792–798.
[46] A. Salimi, E. Sharifi, A. Noorbakhash, S. Soltanian, Electrochem. Commun., 2006, 8, 1499–1508.
[47] A.B. Moghaddam, M.R. Ganjali, R. Dinarvand, S. Ahadi, A.A. Saboury, Biophys. Chem., 2008, 134, 25–33.
[48] A. Mohammadi, A.B. Moghaddam, M. Kazemzad, R. Dinarvand, J. Badraghi, Mater. Sci. Eng. C, 2009, 29, 1752–1758.
[49] M. Miraki, H. Karimi-Maleh, M.A. Taher, S. Cheraghi, F. Karimi, S. Agarwal, V.K. Gupta, J. Mol. Liq., 2019, 278, 672-676.

[50] P. Muthukumaran, C. V.Raju, C. Sumathi, G. Ravi, D. Solairaj, P. Rameshthangam, J. Wilson, S. Rajendran, S. Alwarappan, New J. Chem., 2016, 40, 2741-2748.
[51] D. Han, X. Jing, J. Wang, P. Yang, P.D. Song, J. Liu, J. Electroanal. Chem., 2012, 682, 37–44.
[52] A. Paravannoor, R. Ranjusha, A. M. Asha, R. Vani, S. Kalluri, K.R.V. Subramanian, N. Sivakumar, T.N. Kim, S.V. Nair, A. Balakrishnan, Chem. Eng. J.,2013, 220, 360–366.
[53] H. Dan, C. Ye, Z.M. Lin, S. Chang, Z.C. Xia, X.P. Cheng, J. Electrochem., 2006, 12, 333–336.
[54] G. Hu, C. Tang, C. Li, H. Li, Y. Wang, H. Gong, J. Electrochem. Soc., 2011, 158, A695–A699.
[55] A. J. Bard, L. R. Faulkner, Electrochemical Methods Fundamentals and Applications, 2nd ed. Wiley, New York, 2001.
[56] H. Heli, J. Pishahang, H.B. Amiri, N. Sattarahmady, Microchem. J., 2017, 130, 205-212.
[57] A. Totaganti, S.J. Malode, D.S. Nayak, N.P. Shetti, Mater. Today: Proceedings, 2019, 18, 542-549.
[58] F.F. Hudari, J.C. Souza, M.V.B. Zanoni, Talanta, 2018, 179, 652-657.
[59] A. Jafari-Kashi, M. Shabani-Nooshabadi, Anal. Bioanal. Electrochem., 2018, 10, 1016-1030. [60] C. González-Vargas, N. Serrano, C. Ariño, R. Salazar, M. Esteban, J.M. Díaz-Cruz, Chemosensors, 2017, 5, 25.

How to cite this article:

Sajedeh Salari, Hadi Beitollahi*. Sensitive detection of hydrochlorothiazide using Ce^{3+}/NiO hexagonal nanoparticles modified glassy carbon electrode. Eurasian Chemical Communications, 2021, 3(1), 26-34. Link: http://www.echemcom.com/article_120302.html

Single Crystal X-Ray Structure and DFT-D3 Studies on 2Amino-4-(2,4-Dichlorophenyl)-6-Phenylnicotinonitrile

Zahra Hosseinzadeh[a,*], Mohammad Khavani[b], Ali Ramazani[a,c,*],Hamideh Ahankar[d], Vasyl Kinzhybalo[e]

[a]Department of Chemistry, University of Zanjan, P.O. BOX 4537138791, Zanjan, Iran

[b]Department of Chemistry and Materials Science, School of Chemical Engineering, Aalto University, P.O. BOX 16100, FI-00076 Aalto, Finland

[c]Research Institute of Modern Biological Techniques, University of Zanjan, P.O. BOX 4537138791, Zanjan, Iran

[d]Department of Chemistry, Abhar Branch, Islamic Azad University, P.O. BOX 22, Abhar, Iran

eInstitute of Low Temperature and Structure Research, PAS, 2 Okólna St., 50-422 Wrocław, Poland

*Corresponding Authors: Email - zahra.hosseinzadeh@znu.ac.in & aliramazani@gmail.com, Tel.: +024 33052572,

ABSTRACT

The crystal structure of 2-amino-4-(2,4-dichlorophenyl)-6 phenylnicotinonitrile (ADPN) was determined by single crystal X-ray diffraction. The crystal structure showed two independent molecules with very similar geometric parameters and different environments. Density functional theory (DFT) and DFT dispersion corrected (DFT-D3) calculations were applied to study the structural and chemical properties of ADPN and its dimer. To have a better insight into the properties of the synthesized molecule, quantum chemistry calculations were performed. Based on the calculated results, the dispersion forces have remarkable effects on the stability of ADPN crystal. Moreover, hydrogen bond interactions between ADPN molecules due to molecular orbital interactions can be a driving force for the dimerization process.

KEYWORDS : 2-Amino-4-(2,4-dichlorophenyl) -6-phenylnicotinonitrile; single crystal x-ray structure; DFT-D3; hydrogen bond; quantum chemistry calculation.

INTRODUCTION

Many attempts have been made to develop novel efficient and green synthetic methods for the preparation of heterocyclic compounds because of their high importance in the medicinal science. Heterocyclic compounds with the pyridine scaffold demonstrated a wide variety of biological effects such as antimicrobial, antihypertensive, A2A adenosine receptor antagonizing, cardiovascular, antipyretic, strong inhibitor of HIV-1 integrase, anti-inflammatory, and anti-parkinsonism properties. These multiple pharmaceutical effects have made them interesting synthetic targets. They are also selective inhibitors of IKK-β serine-threonine protein kinase. In fact, these outstanding pharmacophore skeletons are well-known for their biological effects [1-3]. An integral part of numerous natural products such as coenzyme vitamin B6 family and many alkaloids have been formed from the pyridine scaffold [4,5].

In the past decades, multicomponent reactions (MCRs) based on the synthesis of widespread and diverse heterocyclic compounds have been noticed in organic synthesis by chemists and scientists [6-9]. There are several works in the literature concerning the synthesis of 2-amino-4,6-diarylnicotinonitrile derivatives by MCRs [10-13]. We have also synthesized 2-amino-4,6-diarylnicotinonitriles in the

presence of acidic catalysts [14, 15]. We have reported the good cytotoxic activity and the potentiality to bind to the Eg5 binding site (as a validated molecular target) of 2-amino-4-(2,4- dichlorophenyl)-6-phenylnicotinonitrile ADPN) [15]. In the context of our general interest in the synthesis of heterocycle compounds, using single crystal X-ray structure, and DFT studies [16-18], we report the characterization and crystal structure of continuation of ADPN. To have a better insight into the properties of the synthesized molecule, we performed quantum chemistry calculations. As shown in Figure 1, this derivative has been synthesized from the reaction of 2,4-dichlorobenzaldehyde, acetophenone, malononitrile, and ammonium acetate in the presence of boric acid as a green catalyst under microwave irradiation [14]. The structure of the title product 2-amino-4- (2,4-dichlorobenza dichlorophenyl)-6- phenylnicotinonitrile (ADPN) was determined by FT-IR, 1H NMR, and 13C NMR spectroscopic data [14] (See Figures S1 to S3 in Supplementary Information respectively). Moreover, single crystal X-ray analysis was performed in this work.

Preparation of crystals

After recrystallization of the target product from hot ethanol, the pure powder of 2-amino- 4-(2,4-dichlorophenyl)-6- phenylnicotinonitrile (ADPN) was dissolved in hot ethanol. X-ray quality crystals were obtained in excellent yield after slow evaporation of the mother liquor at room temperature.

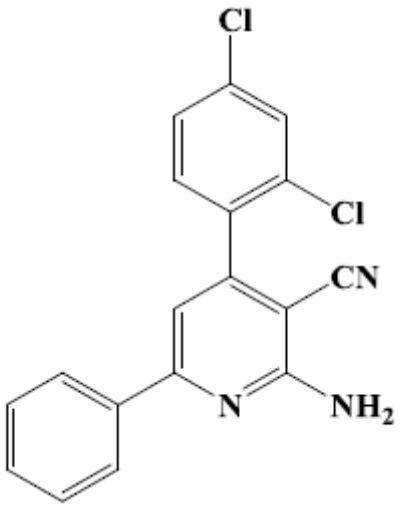

FIGURE 1 Structure of 2-amino-4-(2,4- dichlorophenyl)-6-phenylnicotinonitrile

RESULTS AND DISCUSSION

Density functional theory (DFT) and DFT dispersion corrected (DFT-D3) calculations were used to study the structural and chemical properties of ADPN and its dimer. The structures of ADPN and ADPN dimer were optimized by using BP86 and BP86-D3 functionals with 6-31+G(d) basis set [19, 20]. In order to calculate the thermodynamic parameters during dimerization process frequency calculations were applied. The BP86-D3 functional in contrast to BP86 can describe dispersion interactions; therefore, by employing these functionals, dispersion interactions were calculated.

To investigate the charge transfer and electrostatic interactions inside the ADPN dimer, natural bond orbital (NBO) analysis was performed [21]. By employing NBO analysis, we can study the molecular orbital and donor-acceptor interactions in ADPN dimer. Gaussian 09 computational package was applied for these quantum chemistry calculations [22].

Finally, to determine the nature of interactions between ADPN in dimer structure quantum theory of atoms in molecules (QTAIM) [23], 2D- and 3D-non covalent interaction (NCI) [24] analyses were applied by using MultiWFN 3.4 [25].

X-Ray crystallography

The structure determination of ADPN was carried out on an Oxford Diffraction Xcalibur κ-geometry four-circle diffractometer equipped with an Atlas CCD detector and graphite-monochromated Mo Kα radiation (λ=0.71073 Å). The data collection was carried out at 100(2) K with the use of the Oxford-Cryosystems 800 series cryocooler. Diffraction data were corrected for the polarization and Lorentz effects. Data collection, cell refinement, along with data reduction and analysis were carried out with the CrysAlisPro program package [26]. Analytical shape-based absorption correction was introduced. The crystal structure was solved using SHELXT-2014 [27] and refined by a full-matrix least squares method with the anisotropic thermal parameters for all non-H atoms with the use of SHELXL-2014 [28]. Hydrogen atoms were located in different Fourier maps. In the final refinement cycles, C/N-bound H atoms were put in their calculated positions and refined with a riding model, so that C–H=0.95 Å, N–H=0.88 Å and with Uiso(H)=1.2Ueq(C/N). One of two independent molecules is slightly orientationally disordered, 2,4-dichlorophenyl substituent was split into two positions with the geometry of minor part restricted to be the same as the major. Figures were prepared using the DIAMOND program [29]. The crystallographic information file (CIF) was deposited with The Cambridge Crystallographic Data Centre (http://www.ccdc.cam.ac.uk/; deposition number CCDC 1882629 and published as ESI.

Crystal data for ADPN. C18H11Cl2N3, Mr=340.20, colorless block, crystal dimensions 0.50 × 0.38 × 0.34 mm, monoclinic, sp. gr. P21/c, a=9.421(3), b=27.617(6), c=12.501(4) Å, β=106.31(3)°, V=3121.6(16) $Å^3$, T=100(2) K, Z=8, μ=0.42 mm^{-1} (for Mo Kα, λ=0.71073 Å), analytical shape-based absorption correction, T_{min}=0.89, T_{max}=0.91, 34539 measured reflections, 7849 unique (R_{int} =0.028), 6415 observed (I >2σ(I)), $(\sin \theta/\lambda)_{max}$ = 0.696 Å−1, 448 parameters, 28 restraints, R=0.036, wR = 0.091 (observed refl.), GOOF=S=1.03, $(\Delta\rho_{max})$ = 0.35 and $(\Delta\rho_{min})$=−0.27 e $Å^{-3}$.

The molecular structure of the title compound was confirmed by single-crystal X-ray crystallography. The independent part of the structure and the numbering scheme are shown in Figure 2. It consists of two independent molecules referred to as A and B. Molecule A is slightly disordered over two positions with 2,4-dichlorophenyl ring atoms' occupancies equal to 96.63(12)% and 3.37(12)%, respectively. The geometric parameters of the molecules A and B are quite similar, seeming to be related by a non-crystallographic pseudoinversion center at around (0.49, 0.37, 0.47). The root mean-square distance between respective atoms of overlaid A and inverted B molecules is equal to 0.071 Å (a minor part of the disorder is neglected). The molecule of the title compound consists of three rings: central pyridyl ring, phenyl, and 2,4-dichlorophenyl rings. Average planes fitted to the rings form the following dihedral angles in A and B molecules: 13.35(7)° and 13.48(7)° for ∠(N1/C5, C6/C11), 57.59(9)° and 54.32(7)° for ∠(N1/C5, C13/C18).

Main intermolecular interaction is observed between independent A and B molecules leading to the formation of the dimer by a pair of hydrogen bonds between the amino group hydrogen atom and the nitrogen atom of the nitrile (Figure 3), with the following geometrical parameters: N2A–H2AB···N3B, D–H 0.88 Å, H···A 2.26 Å, D···A 3.0685(19) Å, ∠(D–H···A) 152.2° and N2B–H2BB···N3A D–H 0.88 Å, H···A 2.20 Å, D···A 3.0117(19) Å, ∠(D–H···A) 153.4°. There are no other strong or intermediate

hydrogen bonds in the crystal structure. Above mentioned dimers are further connected by stacking π-π interactions into tetramers: C13B/C18B···(C13B/C18B)^{i} Cg···Cg^{i} 3.81 Å, interplanar distance 3.45 Å, offset 1.62 Å (symmetry code: (i) 1-x, 1-y, 2-z). These tetramers are connected into chains (Figure 3) in an axis direction through Cl···Cl interactions between symmetry related Cl2B atoms: Cl2B···Cl2Bii 3.131 Å (symmetry code: (ii) -x, 1-y, 2-z).

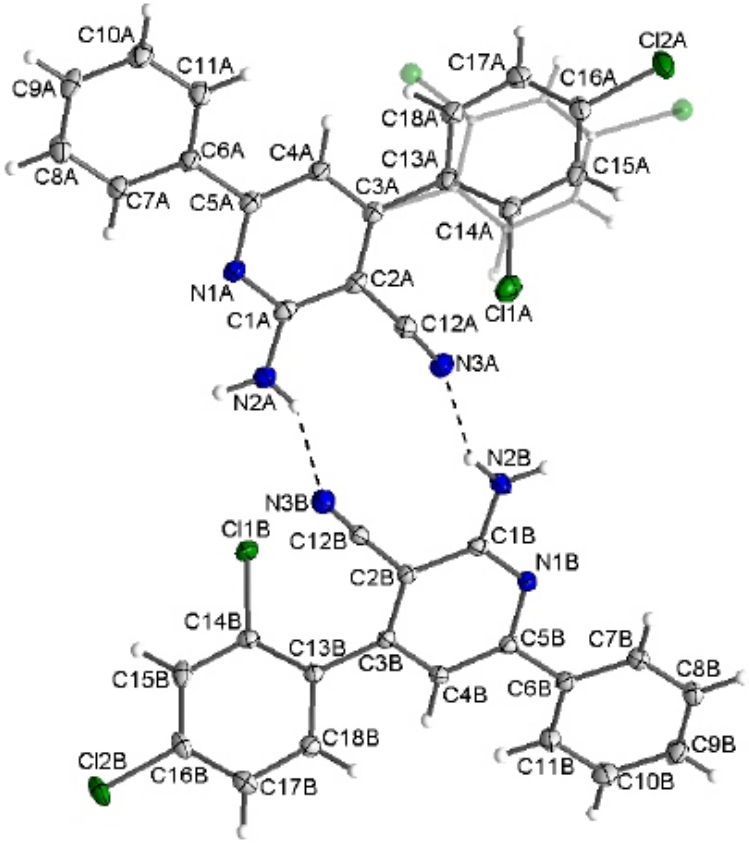

FIGURE 2 Asymmetric part of the structure of 2-amino-4-(2,4-dichlorophenyl)-6-phenylnicotinonitrile along with the numbering scheme. The Minor part of the disordered 2,4-dichlorophenyl ring is shown by transparent lines. Atomic displacement ellipsoids are shown at the 50% probability level

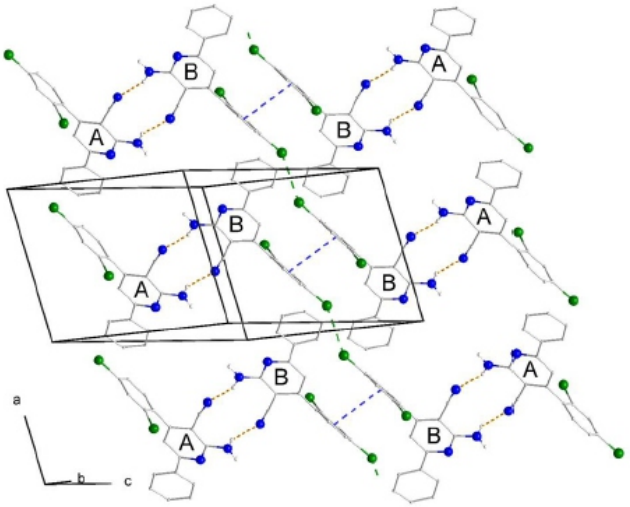

FIGURE 3 Crystal packing of the ADPN structure. The minor part of the disordered 2,4-dichlorophenyl ring and C-bound hydrogen atoms are omitted for clarity. Hydrogen bonds, π-π, Cl···Cl interactions are shown with orange, blue, and green broken lines, respectively

Structural analysis

Figure 4 shows the optimized structures of ADPN and ADPN dimer in the gas phase. According to Table 1, the calculated structural parameters are in good agreement with crystallographic data. For example, the calculated bond lengths for C15–Cl16, C15–C17, C13–H14, C9–C10, and C2–N3 are 1.75, 1.40, 1.09, 1.49 and 1.37 A° and the experimental bond length for the corresponding bonds are 1.73, 1.38, 0.97, 1.48 and 1.35 A°, respectively. Moreover, the calculated H14–C13–C15 and C11–C13–C15 angles by theoretical methods confirmed the experimental values. The calculated values for these angles are 117.75 and 118.79°, which are in good agreement with the experimental results.

Moreover, the structural analysis confirmed the hydrogen bond (H-bond) formation between ADPN in the dimer structure. The calculated N–H bond length of the ADPN monomer is 0.98 A°, which due to dimerization increases to 1.03 A°, confirming a remarkable interaction or H-bond formation between ADPN monomers. To analyze the conformation properties of ADPN dihedral scan calculation for C6/C9/C10/C11 angle was applied. According to the obtained results, there are three structural conformers for ADPN, as shown in Figure S4 in Supplementary Information. Based on the calculated energies, the conformer 2 (Figure S4) has the most stable structure, which is consistent with the crystallographic data. Moreover, NMR calculations were employed at the BP86/6-13G(d) level of theory. The calculated NMR spectra (see supporting information) clearly show the difference in geometrical properties for the ADPN.

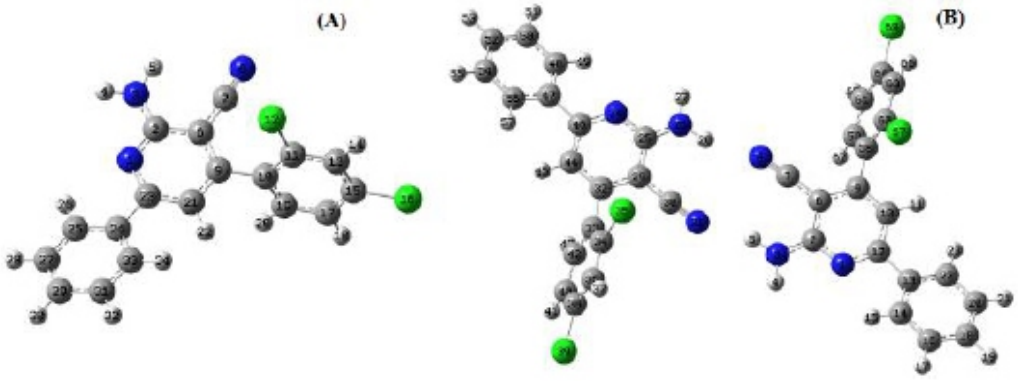

FIGURE 4 The optimized structures of ADPN monomer (A) and its dimer (B) with atom numbering at BP86/6-31+G(d) level of theory

TABLE 1 The calculated geometrical parameters of ADPN and its dimer at BP86/6-31+G(d) level of theory (bonds and angles are in A° and degree, respectively)

Monomer			Dimer		
Parameters	Theory	Experimental	Parameters	Theory	Experimental
C15–Cl16	1.75	1.73	H28···N8	2.02	2.19
C17–C15	1.40	1.38	N31···H5	2.02	2.26
C13–H14	1.09	0.97	C8–N7	1.17	1.14
C9–C10	1.49	1.48	N3–H5	1.02	0.93
C7–N8	1.18	1.15	C2–C6	1.44	1.42
C2–N3	1.37	1.35	C7–N8···H28	161.70	157.90
Cl12–C11–C13	117.75	117.04	C6–C2–C29	79.34	81.50
H14–C13–C15	120.88	120.72	C7–C6–C2	119.73	118.06
C11–C13–C15	118.79	118.59	C26–C25–C29	122.03	121.82
C9–C10–C11	123.02	124.50	H28–H5–N3	146.20	157.86
C6–C9–C10–C11	73.40	57.68	C29–C30–C7–C6	174.72	171.85

Table 2 shows the thermodynamic parameters of the ADPN dimerization process. Calculated values of binding energy (ΔE), enthalpy energy (ΔH), and Gibbs energy (ΔG) by BP86-D3 functional are greater than those from BP86 functional, which confirms an important contribution of dispersion forces. According to Table 2, the negative values of ΔE show the considerable stability of ADPN dimer and the negative values of ΔH reveal that the dimerization process is exothermic. Moreover, the calculated values of ΔG by different functionals confirmed that the dimerization process is favorable from the thermodynamic point of view.

TABLE 2 The calculated thermodynamic parameters (kcal·mol-1) of the ADPN dimerization process by different functionals

	ΔE	ΔH	ΔG
BP86	-7.53	-8.13	-1.77
BP86-D3	-15.56	-16.15	-3.36
	ΔE_{dis}	ΔH_{dis}	ΔG_{dis}
(BP86-D3)-BP86	-8.03	-8.02	-1.59

The calculated dispersion binding energy (ΔEdis) for the dimerization process is -8.03 kcal·mol^{-1}. According to the structural analysis, each dimer can form two N–H···N bonds, so the H-bond interaction energy for each bond is -4.01 kcal·mol^{-1}. These results are in good agreement with the reported values in the literature [30]. It is well worth mentioning that the negative values of the calculated dispersion thermodynamic parameters reveal that dispersion forces have a considerable role in the crystal stability of ADPN.

Quantum reactivity indices and molecular orbital interaction

To investigate the electrostatic and donor−acceptor interactions between ADPN in dimer structure, we did NBO analysis. By employing this method, stabilization energy values, E(2), were calculated. Using the NBO method, it is possible to find related information about the interactions of orbitals. Second-order perturbation theory analysis was employed to calculate the donor−acceptor interactions. In this analysis, the stabilization energy, E(2), is related to the molecular orbital interactions; when the E(2) energy between a donor and an acceptor group is large, there is a strong interaction. For each donor orbital (i) and acceptor orbital (j), E(2) is associated with i →j delocalization and is given by equation 1:

$$E(2)= \Delta E_{i,j}= q_i \{F^2 (i,j) / (E_j - E_i)\} \quad (1)$$

where q_i is the i^{th} donor orbital occupancy, E_i and E_j are diagonal elements, and (i,j) are off-diagonal elements of the Fock matrix.

Table 3 shows the most important donor-acceptor interactions between lone pair (Lp) electrons of N atoms and bonding orbitals (σ and π) as a donor with antibonding orbitals (σ* and π*) of different bonds as an acceptor. The calculated E(2) values for the ADPN monomer shows strong orbital interactions between bonding orbitals of N1–C2 bond (πN1C2) with antibonding orbital of C21–C23 bond (π^*_{C21C23}). In dimer structure, there are considerable orbital interactions for $\pi_{C2C6} \rightarrow \pi^*_{C7N8}$, $\pi_{C2C6} \rightarrow \pi^*_{C9C10}$, $\pi_{N1C12} \rightarrow \pi^*_{C2C6}$. The calculated E(2) values for the interaction between LP electrons of N8 and N31 atoms with an antibonding orbital of N26–H28 and N3–H5 bond, respectively, confirming H-bond formation between ADPN monomers. In other words, the origin of the dimer stability is H–bond formation because of strong molecular orbital interactions between (Lp) electrons of N atoms and σ^*_{NH} orbitals.

To investigate the reactivity of ADPN and its dimer, the HOMO-LUMO analysis was applied. Based on the HOMO and LUMO, we can describe the reactivity of a molecule. E_H and E_L are HOMO and LUMO energies, respectively. The lower value of ELUMO, indicates that the molecule would accept electrons. Figure 5 shows the HOMO and LUMO diagrams of ADPN and its dimer. According to Figure 5, the HOMOs locate on heteroatoms of ADPN, while LUMOs show a contrast pattern. In other words, LUMOs extend to the whole molecule in comparison to HOMOs, especially for the dimer structure.

TABLE 3 The calculated E(2) values (kcal·mol^{-1}) for different donor- acceptor interactions at BP86/6-31+G(d) level of theory

Monomer		Dimer	
Donor →Acceptor	E(2)	Donor →Acceptor	E(2)
$\pi_{C2N3} \rightarrow \pi^*_{N1C23}$	2.18	$\sigma_{C2N3} \rightarrow \pi^*_{N1C12}$	2.12
$\pi_{C2C6} \rightarrow \pi^*_{N3H4}$	1.94	$\pi_{C2C6} \rightarrow \pi^*_{C7N8}$	21.44
$\sigma_{N3H4} \rightarrow \pi^*_{C2C6}$	4.53	$\pi_{C2C6} \rightarrow \pi^*_{C9C10}$	20.17
$\pi_{C6C7} \rightarrow \pi^*_{C7N8}$	3.66	$\sigma_{N3H5} \rightarrow \pi^*_{N1C2}$	4.25
$\pi_{N1C2} \rightarrow \pi^*_{C21C23}$	21.91	$\pi_{N1C12} \rightarrow \pi^*_{C2C6}$	23.76
$\pi_{N1C23} \rightarrow \pi^*_{C2N3}$	3.53	$\pi_{N1C126} \rightarrow \pi^*_{C9C10}$	7.09
$\pi_{C6C9} \rightarrow \pi^*_{C2N3}$	3.08	$\pi_{N1C12} \rightarrow \pi^*_{C13C22}$	7.22
$\pi_{C6C9} \rightarrow \pi^*_{C2C6}$	3.08	$\pi_{C9C10} \rightarrow \pi^*_{N1C12}$	21.70
$Lp_{N1} \rightarrow \sigma^*_{C2N3}$	3.08	$\pi_{C9C10} \rightarrow \pi^*_{C2C6}$	9.57
$Lp_{N1} \rightarrow \pi^*_{C2C6}$	10.43	$Lp_{N8} \rightarrow \pi^*_{N26H28}$	11.93
$Lp_{N1} \rightarrow \pi^*_{C21C23}$	8.96	$Lp_{N31} \rightarrow \pi^*_{N3H5}$	12.04

According to Table 4, due to dimerization EL and EH values decrease and dimer structure has a lower band gap (ΔE_{L-H}) in comparison to the ADPN monomer. This result indicates that the dimerization increases the reactivity of the ADPN molecule. Moreover, the calculated chemical potential (μ) reveals that dimerization process elevates the stability of ADPN, which is according to the calculated thermodynamic parameters. Based on the calculated electrophilicity index (ω) values for monomer and dimer structure, dimer has a lower electron affinity in comparison to monomer. Actually, the charge transfer between ADPN molecules can be a reason for decreasing the electron affinity.

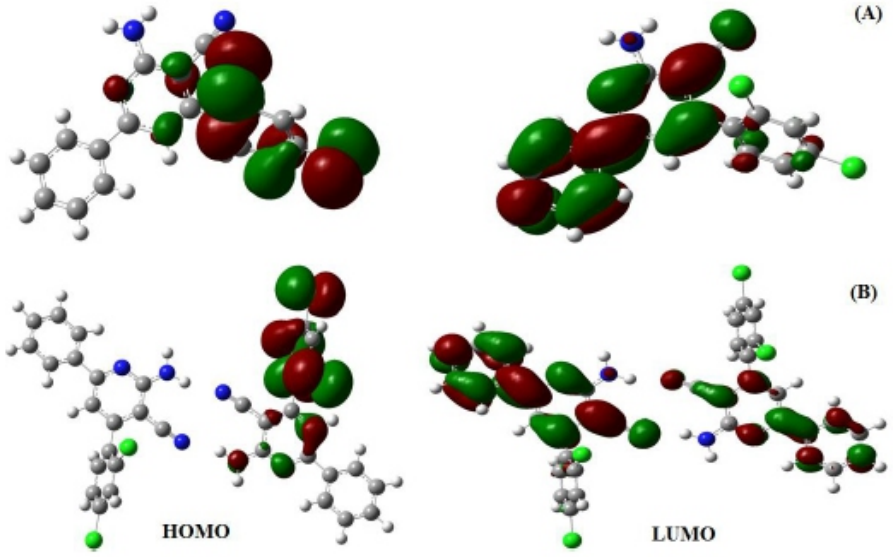

FIGURE 5 The HOMO and LUMO diagrams of ADPN (A) and its dimer (B) at BP86/6-31+G(d) level of theory

TABLE 4 The calculated quantum reactivity indices (eV) of ADPN and its dimer at BP86/6-31+G(d) level of theory

	E_L	E_H	ΔE_{L-H}	μ	ω
Monomer	-3.00	-5.78	2.78	-4.39	3.46
Dimer	-2.92	-5.48	2.56	-4.20	3.44

Topological and NCI analysis

To investigate the nature of the interaction between the ADPN molecules in dimer structure, we obtained topological parameters of the H-bonds by applying QTAIM analysis (Table 5). This method calculates the topological parameters at the bond critical points (BCPs). The value of electron density (ρ) at the BCP shows the strength of a given bond. Laplacian (L(r)) represents the curvature of the electron density in a three-dimensional space at the BCP of the atomic interaction. Generally, a negative value of Laplacian shows covalent interactions, while a positive Laplacian confirms the electrostatic interactions. If the ratio of the kinetic energy density (G) and potential energy density (V) (-G/V) is less than 0.5, the interaction is covalent. When the ratio is between 0.5 and 1, the interaction is partly covalent. If the −G/V ratio is greater than 1, the interactions are non-covalent. Therefore, by applying the ratio of –G/V, we can determine the nature of the interactions.

According to Table 5, the calculated ρ of the N3–H5 bond is higher than N8···H28 interaction. In other words, internal interactions are stronger than those of external. The calculated negative values of Laplacian for N3–H5 and N26–H28 bonds reveals a covalent character for these bonds. Moreover, the calculated –G/V ratios for N8···H28 and N3–H5 interactions are greater than 1.0, confirming H-bond formation between ADPN molecules.

TABLE 5 The calculated topological parameters at the BCP of the ADPN dimer at BP86/6-31+G(d) level of theory

Bonds	ρ	L(r)	-G/V
N8···H28	0.0231	0.0744	1.05
N31···H5	0.0232	0.0746	1.05
N26–H28	0.3092	-0.1537	0.8214
N3–H5	0.3092	-0.1536	0.8293

By employing NCI analysis, it is possible to determine the nature of the interactions based on electron density and the sign of the second derivative in the perpendicular direction of the bond (λ_2). The NCI analysis provides a 2D plot of the reduced density gradient, RDG, in which the sign of λ2 shows the nature of the interaction.

The $-\lambda_2$ confirms a bonding interaction, such as hydrogen bonds, whereas $+\lambda_2$ shows nonbonding interactions and van der Waals (vdW) interactions can be determined by negligible values of λ_2.

According to Figure 6-A, the red, green, and blue ovals indicate repulsion interactions, vdW, and H-bond, respectively. The $-\lambda_2$ (Figure 6-A), confirms H-bond formation between ADPN molecules. Moreover, a 3D- NCI plots were applied, which is also represented in Figure 6-B. In this plot, the blue, red, and green isosurfaces reveal H-bond, repulsive, and vdW interactions, respectively

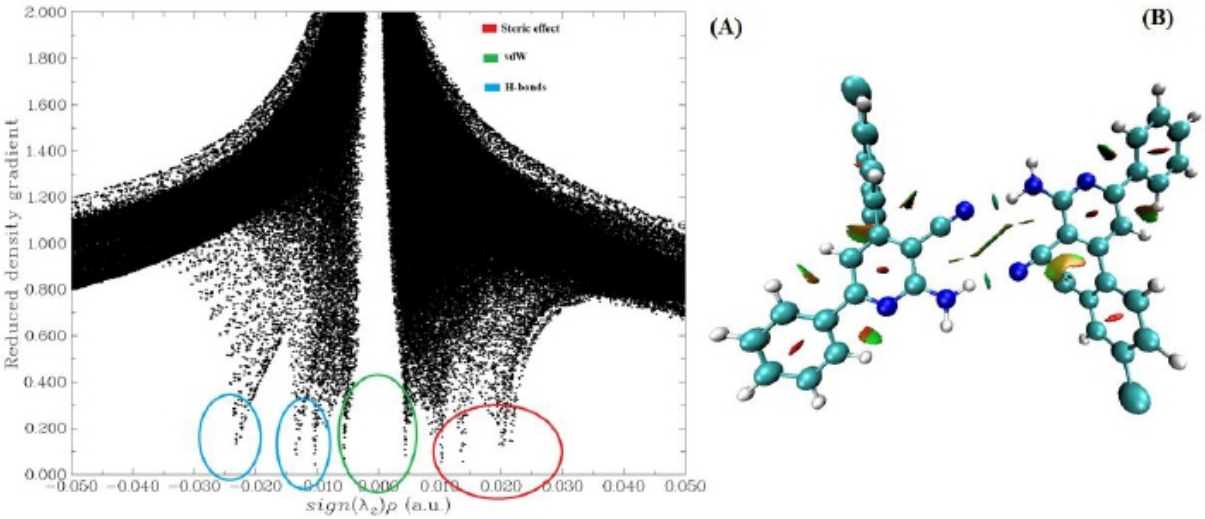

FIGURE 6 The 2D- (A) and 3D-NCI (B) plots of the ADPN dimer

According to Figure 6-B, the blue isosurfaces between CN and NH groups confirm H-bond interactions between ADPN molecules. And green isosurfaces between N atoms of the ring and CH groups reveal a considerable vdW interaction inside the ADPN molecules. NCI analysis reveals that H-bond formation between ADPN molecules is one of the important factors on the stability of dimer structure.

CONCLUSION

In summary, we prepared single crystal of 2-amino-4-(2,4-dichlorophenyl)-6-phenylnicotinonitrile (ADPN) and characterized it by X-ray single crystal diffraction. Quantum chemistry calculations were applied by using different functionals to investigate the structural and chemical properties of ADPN and its dimer. The calculated structural parameters are in good agreement with experimental data and the obtained dispersion parameters confirmed that dispersion forces have a considerable role in the stability of ADPN crystal. Based on the obtained results from DFT calculations, the nature of the interactions was determined, which can provide remarkable information about the structural features of the reported compound. Moreover, NCI analysis revealed that H-bond formation between ADPN is a driving force for the dimerization process and the main origin of this interaction is donor-acceptor interaction between molecular orbitals.

ACKNOWLEDGMENTS

The authors greatly appreciate the University of Zanjan, Iran, for its support

Orcid:

Ali Ramazani: https://orcid.org/0000-0003-3072-7924

Hamideh Ahankar: https://orcid.org/0000-0002-2717-8920

REFERENCES

[1] A. Sutherland, T. Gallagher, C.G. Sharples, S. Wonnacott, J. Org. Chem., 2003, 68, 2475-2478.
[2] N.D. Cosford, L. Tehrani, J. Roppe, E. Schweiger, N.D. Smith, J. Anderson, L. Bristow, J. Brodkin, X. Jiang, I. McDonald, J. Med. Chem., 2003, 46, 204-206.
[3] I.J. Enyedy, S. Sakamuri, W.A. Zaman, K.M. Johnson, S. Wang, Bioorg. Med. Chem. lett., 2003, 13, 513-517.

[4] F.W. Lichtenthaler, Acc. Chem. Res., 2002, 35, 728-737.
[5] V.P. Litvinov, Russ. Chem. Rev., 2003, 72, 69-85.
[6] H. Aghahosseini, A. Ramazani, Eurasian Chem. Commun., 2020, 2, 410-419.
[7] S. Sajjadifar, M.A. Zolfigol, G. Chehardoli, Eurasian Chem. Commun., 2020, 2, 812-818.
[8] F. Mostaghni, F. Taat, Eurasian Chem. Commun., 2020, 2, 427-432.
[9] M. Rohaniyan, A. Davoodnia, A. Khojastehnezhad, S.A. Beyramabadi, Eurasian Chem. Commun., 2020, 2, 329-339.
[10] S.S. Mansoor, K. Aswin, K. Logaiya, P.N. Sudhan, S. Malik, Res. Chem. Intermed., 2014, 40, 871-885.
[11] H.C. Shah, V.H. Shah, N.D. Desai, Arkivoc, 2009, 2, 76-87.
[12] K. Niknam, R. Rashidian, A. Jamali, Sci. Iran., 2013, 20, 1863-1870.
[13] H. Karimi, Iran. J. Chem. Chem. Eng. (IJCCE), 2017, 36, 11-19.
[14] Z. Hosseinzadeh, A. Ramazani, N. Razzaghi-Asl, K. Slepokura, T. Lis, Turk. J. Chem., 2019, 43, 464-474.
[15] Z. Hosseinzadeh, N. Razzaghi-Asl, A. Ramazani, H. Aghahosseini, A. Ramazani, Turk. J. Chem., 2020, 44, 194-213.
[16] A. Ramazani, M. Sheikhi, H. Ahankar, M. Rouhani, S.W. Joo, K. Ślepokura, T. Lis, J. Chem. Crystallogr., 2017, 47, 198-207.
[17] A. Ramazani, H. Ahankar, K. Ślepokura, T. Lis, P.A. Asiabi, M. Sheikhi, F. Gouranlou, H. Yahyaei, J. Chem. Crystallogr., 2020, 50, 99-113.
[18] A. Ramazani, M. Sheikhi, Y. Hanifehpour, P. Asiabi, S. Joo, J. Struct. Chem., 2018, 59, 529-540.
[19] H.-B. Chen, Y. Zhao, Y. Liao, RSC Adv., 2015, 5, 37737-37741.
[20] T. Risthaus, S. Grimme, J. Chem. Theory Comput., 2013, 9, 1580-1591.
[21] A.E. Reed, L.A. Curtiss, F. Weinhold, Chem. Rev., 1988, 88, 899-926.
[22] M. Frisch, G. Trucks, H. Schlegel, G. Scuseria, M. Robb, J. Cheeseman, G. Scalmani, V. Barone, B. Mennucci, G. Petersson, Wallingford, CT, 2009, 32, 5648-5652.
[23] R. Bader, Atoms in Molecules: A Quantum Theory, Oxford University, New York., 1990.
[24] R. Chaudret, B. De Courcy, J. Contreras-Garcia, E. Gloaguen, A. Zehnacker-Rentien, M. Mons, J.-P. Piquemal, Phys. Chem. Chem. Phys, 2014, 16, 9876-9891.
[25] T. Lu, F. Chen, J. Comput. Chem., 2012, 33, 580-592.
[26] CrysAlisCCD and CrysAlisRED in KM4-CCD software. Oxford Diffraction Ltd.: Abingdon, England 2010
[27] G.M. Sheldrick, Acta Crystallogr. Sect. A: Found. Crystallogr., 2015, 71, 3-8.
[28] G.M. Sheldrick, Acta Crystallogr., Sect. C: Struct. Chem., 2015, 71, 3-8.
[29] K. Brandenburg, DIAMOND Version 3.2k. Crystal Impact GbR: Bonn, Germany, 2014
[30] J. Emsley, Chem. Soc. Rev., 1980, 9, 91-124.

How to cite this article:

Zahra Hosseinzadeh*, Mohammad Khavani Sariani, Ali Ramazani*, Hamideh Ahankar, Vasyl Kinzhybalo. Single crystal X-Ray structure and DFT-D3 studies on 2-amino-4-(2,4-dichlorophenyl)-6-phenylnicotinonitrile. Eurasian Chemical Communications, 2021, 3(1), 35-44. Link: http://www.echemcom.com/article_120553.html

Instructions for Authors

Essentials for Publishing in this Journal

1 Submitted articles should not have been previously published or be currently under consideration for publication elsewhere.

2 Conference papers may only be submitted if the paper has been completely re-written (taken to mean more than 50%) and the author has cleared any necessary permission with the copyright owner if it has been previously copyrighted.

3 All our articles are refereed through a double-blind process.

4 All authors must declare they have read and agreed to the content of the submitted article and must sign a declaration correspond to the originality of the article.

Submission Process

All articles for this journal must be submitted using our online submissions system. http://enrichedpub.com/ . Please use the Submit Your Article link in the Author Service area.

Manuscript Guidelines

The instructions to authors about the article preparation for publication in the Manuscripts are submitted online, through the e-Ur (Electronic editing) system, developed by **Enriched Publications Pvt. Ltd**. The article should contain the abstract with keywords, introduction, body, conclusion, references and the summary in English language (without heading and subheading enumeration). The article length should not exceed 16 pages of A4 paper format.

Title

The title should be informative. It is in both Journal's and author's best interest to use terms suitable. For indexing and word search. If there are no such terms in the title, the author is strongly advised to add a subtitle. The title should be given in English as well. The titles precede the abstract and the summary in an appropriate language.

Letterhead Title

The letterhead title is given at a top of each page for easier identification of article copies in an Electronic form in particular. It contains the author's surname and first name initial .article title, journal title and collation (year, volume, and issue, first and last page). The journal and article titles can be given in a shortened form.

Author's Name

Full name(s) of author(s) should be used. It is advisable to give the middle initial. Names are given in their original form.

Contact Details

The postal address or the e-mail address of the author (usually of the first one if there are more Authors) is given in the footnote at the bottom of the first page.

Type of Articles

Classification of articles is a duty of the editorial staff and is of special importance. Referees and the members of the editorial staff, or section editors, can propose a category, but the editor-in-chief has the sole responsibility for their classification. Journal articles are classified as follows:

Scientific articles:

1. Original scientific paper (giving the previously unpublished results of the author's own research based on management methods).

2. Survey paper (giving an original, detailed and critical view of a research problem or an area to which the author has made a contribution visible through his self-citation);

3. Short or preliminary communication (original management paper of full format but of a smaller extent or of a preliminary character);

4. Scientific critique or forum (discussion on a particular scientific topic, based exclusively on management argumentation) and commentaries. Exceptionally, in particular areas, a scientific paper in the Journal can be in a form of a monograph or a critical edition of scientific data (historical, archival, lexicographic, bibliographic, data survey, etc.) which were unknown or hardly accessible for scientific research.

Professional articles:

1. Professional paper (contribution offering experience useful for improvement of professional practice but not necessarily based on scientific methods);
2. Informative contribution (editorial, commentary, etc.);
3. Review (of a book, software, case study, scientific event, etc.)

Language

The article should be in English. The grammar and style of the article should be of good quality. The systematized text should be without abbreviations (except standard ones). All measurements must be in SI units. The sequence of formulae is denoted in Arabic numerals in parentheses on the right-hand side.

Abstract and Summary

An abstract is a concise informative presentation of the article content for fast and accurate Evaluation of its relevance. It is both in the Editorial Office's and the author's best interest for an abstract to contain terms often used for indexing and article search. The abstract describes the purpose of the study and the methods, outlines the findings and state the conclusions. A 100- to 250-Word abstract should be placed between the title and the keywords with the body text to follow. Besides an abstract are advised to have a summary in English, at the end of the article, after the Reference list. The summary should be structured and long up to 1/10 of the article length (it is more extensive than the abstract).

Keywords

Keywords are terms or phrases showing adequately the article content for indexing and search purposes. They should be allocated heaving in mind widely accepted international sources (index, dictionary or thesaurus), such as the Web of Science keyword list for science in general. The higher their usage frequency is the better. Up to 10 keywords immediately follow the abstract and the summary, in respective languages.

Acknowledgements

The name and the number of the project or programmed within which the article was realized is given in a separate note at the bottom of the first page together with the name of the institution which financially supported the project or programmed.

Tables and Illustrations

All the captions should be in the original language as well as in English, together with the texts in illustrations if possible. Tables are typed in the same style as the text and are denoted by numerals at the top. Photographs and drawings, placed appropriately in the text, should be clear, precise and suitable for reproduction. Drawings should be created in Word or Corel.

Citation in the Text

Citation in the text must be uniform. When citing references in the text, use the reference number set in square brackets from the Reference list at the end of the article.

Footnotes

Footnotes are given at the bottom of the page with the text they refer to. They can contain less relevant details, additional explanations or used sources (e.g. scientific material, manuals). They cannot replace the cited literature.
The article should be accompanied with a cover letter with the information about the author(s): surname, middle initial, first name, and citizen personal number, rank, title, e-mail address, and affiliation address, home address including municipality, phone number in the office and at home (or a mobile phone number). The cover letter should state the type of the article and tell which illustrations are original and which are not.

Address of the Editorial Office:

Enriched Publications Pvt. Ltd.
S-9,IInd FLOOR, MLU POCKET,
MANISH ABHINAV PLAZA-II, ABOVE FEDERAL BANK,
PLOT NO-5, SECTOR -5, DWARKA, NEW DELHI, INDIA-110075,
PHONE: - + (91)-(11)-45525005